NATIONAL TECHNICAL UNIVERSITY OF ATHENS
SCHOOL OF CIVIL ENGINEERING
DEPARTMENT OF GEOTECHNICAL ENGINEERING

STATIC ANALYSIS OF THE STABILITY OF THE LEANING TOWER OF PISA

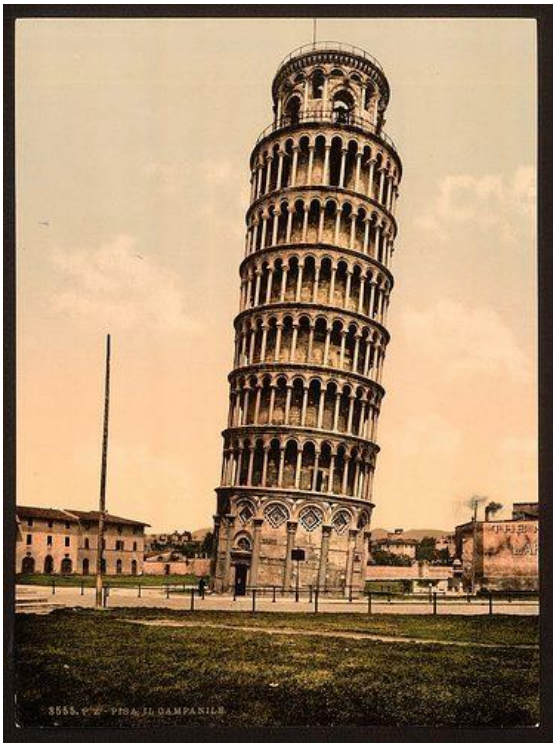

Diploma Thesis

Maria Plota

Supervisor: Professor George Gazetas

Athens, March 2018

NATIONAL TECHNICAL UNIVERSITY OF ATHENS
SCHOOL OF CIVIL ENGINEERING
DEPARTMENT OF GEOTECHNICAL ENGINEERING

DIPLOMA THESIS

STATIC ANALYSIS OF THE STABILITY OF THE LEANING TOWER OF PISA

Maria Plota

Supervisor: Professor George Gazetas
March 2018

Στους γονείς μου
και τα αδέρφια μου

ΕΥΧΑΡΙΣΤΙΕΣ

Φτάνοντας στο πέρας των προπτυχιακών μου σπουδών στο Εθνικό Μετσόβιο Πολυτεχνείο, ένα στόχο σταθμό στη ζωή μου, θα ήθελα από καρδιάς να ευχαριστήσω τα πρόσωπα εκείνα που με στήριξαν πνευματικά και ηθικά σε όλο το διάστημα των σπουδών μου, καθώς και τους ανθρώπους που συνέβαλαν σημαντικά στην εκπόνηση της διπλωματικής μου εργασίας.

Πρώτα από όλα θα ήθελα να ευχαριστήσω τον καθηγητή μου, κ. Γεώργιο Γκαζέτα, για την έμπνευση και τα κίνητρα που προσέφερε σε όλους μας ήδη από τη διδασκαλία των μαθημάτων στις αίθουσες, κάνοντάς μας να αγαπήσουμε τον τομέα της Γεωτεχνικής Μηχανικής, καθώς και για την ευκαιρία που μου έδωσε να συνεργαστώ μαζί του στα πλαίσια της διπλωματικής μου εργασίας. Μέσα από την επικοινωνία μας, τη συμπαράστασή του και τη μετάδοση των γνώσεών του στάθηκε αρωγός σε μια απαιτητική και προσοδοφόρα περίοδο της ζωής μου.

Αμέριστη ήταν, επίσης, η βοήθεια και η συμπαράσταση της δρ. Ευαγγελίας Γαρίνη. Διαθέτοντας το χρόνο, τις γνώσεις και την καλή της διάθεση ανά πάσα στιγμή με βοήθησε σημαντικά να ξεπεράσω τις όποιες δυσκολίες προέκυπταν και για αυτό την ευχαριστώ θερμά.

Κλείνοντας, ευχαριστώ πάρα πολύ την οικογένειά μου, σταθερό παραστάτη στις αγωνίες, τις χαρές και την προσπάθειά μου όλα αυτά τα χρόνια, καθώς και τους αγαπημένους μου φίλους και τους συντρόφους του σχήματος Αν.Αρ.Πα-Ε.Α.Α.Κ που με τη στήριξη και τη συλλογική δουλειά με βοήθησαν να πετύχω τους στόχους μου.

Σας ευχαριστώ!

ΠΕΡΙΛΗΨΗ

Στην παρούσα διπλωματική εργασία αναλύουμε την ευστάθεια του Πύργου της Πίζας και ερευνάμε τη μηχανική συμπεριφορά του υπεδάφους του. Ο Πύργος της Πίζας αποτελεί εδώ και χρόνια ιδιαίτερη πρόκληση στον τομέα της γεωτεχνικής μηχανικής, καθώς έχει θεμελιωθεί σε ένα αδύναμο και αρκετά συμπιεστό έδαφος, ενώ την ίδια στιγμή η κλίση του αυξάνεται συνεχώς μέχρι τη σημερινή του κατάσταση. Το φαινόμενο αστάθειας λόγω της κλίσης του Πύργου είναι αυτό που ελέγχει τη συμπεριφορά του κτιρίου και γίνεται καλύτερα κατανοητό μέσα από την ιστορία της κατασκευής και της συνακόλουθης κλίσης του.

Εκτεταμένες γεωτεχνικές έρευνες πραγματοποιήθηκαν κατά τις διάφορες εκστρατείες, με στόχο το σχεδιασμό και την εφαρμογή μέτρων για τη σταθεροποίηση του κτιρίου, και οδήγησαν στην απόκτηση μιας μεγάλης βάσης δεδομένων αναφορικά με τις φυσικές και μηχανικές ιδιότητες του υπεδάφους του Πύργου. Πραγματοποιούμε μια συνοπτική παρουσίαση των γεωτεχνικών χαρακτηριστικών του εδάφους, ώστε να κατανοήσουμε καλύτερα την απόκρισή του στα επιβαλλόμενα φορτία που προέρχονται από την ανωδομή και να προσδιορίσουμε τα δεδομένα που χρειάζονται για την ανάλυση του προβλήματός μας.

Το σύστημα του Πύργου της Πίζας κα του υπεδάφους του μοντελοποιήθηκαν με αριθμητική προσομοίωση πεπερασμένων στοιχείων και οι αναλύσεις έγιναν με το πρόγραμμα Abaqus. Πραγματοποιήσαμε στατικές αναλύσεις, ώστε να ελέγξουμε τη σωστή συμπεριφορά του μοντέλου μας, να προσομοιώσουμε κατά το δυνατόν καλύτερα τη σημερινή κατάσταση του Πύργου και να ερμηνεύσουμε την απόκριση του εδάφους υπό το βάρος της ανωδομής και τη ροπή ανατροπής λόγω της κλίσης του κτιρίου. Για την επίτευξη του σκοπού αυτού, εκτελέσαμε τόσο ελαστικές αναλύσεις όσο και αναλύσεις χρησιμοποιώντας ως καταστατικό μοντέλο πλαστικοποίησης του εδάφους το μοντέλο Mohr-Coulomb. Προσπαθήσαμε να πετύχουμε μια ρεαλιστική εκτίμηση της ροπής αντοχής του εδάφους, ώστε να εξηγείται επαρκώς η ευστάθεια του Πύργου στις επκρατούσες συνθήκες. Τα αποτελέσματα παρουσιάζονται κατά βάση με τη

μορφή διαγραμμάτων ροπής-στροφής, τάσεων και καθιζήσεων του εδάφους κάτω από το θεμέλιο, για την καλύτερη κατανόηση της σημερινής κατάστασης του Πύργου.

ABSTRACT

In this diploma thesis we analyze the stability of the Leaning Tower of Pisa and investigate the mechanical behavior of its subsoil. The Tower of Pisa has been a very difficult challenge for geotechnical engineering, since it is founded on weak, highly compressible soil and its inclination has been increasing inexorably over the years to the point at which is standing today. The phenomenon of leaning instability controls the behavior of the building and the history of its construction and inclination are significant for the better comprehension of this phenomenon.

Extensive geotechnical investigations that were performed during campaigns for the design and implementation of measures for the safety of the building led to a big amount of information regarding the physical and mechanical properties of the subsoil lying beneath the Tower. A synopsis of the geotechnical characteristics of the subsoil is attempted herein, so as to better understand its response to the loads applied due to the superstructure of the Tower, as well as determine the data needed as input for the following analysis.

The system of the Tower of Pisa and its subsoil is modeled with numerical finite elements and analyzed with the Abaqus code. Static analyses have been carried out, in order to confirm the validity of our model, reach the current condition of the Tower and interpret the response of its subsoil under the weight of the building and the overturning moment generated due to its inclination. To this end, we have performed both elastic analysis and analysis assuming Mohr-Coulomb plastic behavior of the subsoil. We tried to achieve a realistic assessment of the resisting moment generated be the rotational stiffness of the subsoil that adequately explains the stability of the Tower. The results are presented mainly in the form of rotation, stresses and displacements under the footing, so as to better understand the current state of the Tower.

Table of Contents

CHAPTER 1
INTRODUCTION AND LITERATURE REVIEW

1.1 HISTORY

The Tower of Pisa is one of the most popular and admirable sights worldwide. Founded in August 1173, the building is the bell tower of the cathedral complex of Piazza dei Miracoli (Square of Miracles shown in figure 1.1), located in the city of Pisa (Tuscany, Italy). The square is dominated by four religious edifices: the Pisa Cathedral, the Pisa Baptistry, The Campanile and the Camposanto Monumentale and is recognized as an important center of European medieval art. The construction of the complex begun in 1064, during the rise of Pisa to a mighty maritime nation, in order to demonstrate the power of the Republic and was significantly funded by the booty taken from the island of Majorca in the 12th century.

The inadequate foundation of the Tower set in a soil that contains soft layers and deposits which differ considerably over short horizontal distances led to the leaning of the building from the first period of its construction. The excessive inclination of the Tower caused by its continuous movement over the years and the collapse of the San Marco Bell Tower in Venice in the early 20th century pointed out the need for stabilization measures to be taken. A number of Commissions were set up by the Ministries of Instruction and Public Works and several interventions were proposed, but no action was actually taken. The sudden collapse of the Civic Tower in Pavia in 1989 again drew attention to the leaning Tower of Pisa, since it signalized the risk of collapse not only due to foundation failure, but also due to brittle failure of the masonry. The Tower doors were closed to visitors in January 1990 and the Prime Minister set up an International Committee for the Safeguard of the Tower of Pisa in March. The Committee was authorized to conceive, design and implement the interventions needed to both stabilize the Tower and restore the

monument surfaces. The final interventions were carried out in the 1998-2001 period and the Tower was again opened to the public in December 2001.

1.2 TIMELINE OF CONSTRUCTION AND CONSEQUENT INCLINATION

The construction of the Tower began in 1173 and had progressed to half way up the fourth order by 1178, when the work was interrupted for unknown reasons, preventing though the foundations from experiencing an undrained bearing capacity failure. The work was recommenced in 1272, after a pause of nearly 100 years, by which time the strength of the ground had increased due to consolidation under the weight of the structure. By about 1278, construction had reached the seventh cornice when work was again stopped. Once again had work continued, the Tower of Pisa would have fallen over. In about 1360, work on the bell chamber was commenced and was completed in about 1370, two centuries after the work had been started. The construction history is depicted in figure 1.2.

A reliable clue to the history of the tilt lies in the adjustments made to the masonry layers during construction and in the resulting shape of the axis of the Tower, shown in figure 1.3. According to both this shape and a hypothesis on the manner in which the masons corrected the progressive inclination of the Tower (BURLAND, VIGGIANI 1994), the history of inclination can be deduced as illustrated in figure 1.4. To be more specific, during the first phase of construction, to just above the third cornice, the Tower inclined slightly to the north and, after the rest period, the northward inclination had increased to about 0.2˚. When construction was recommenced the building started leaning southwards and accelerated shortly before construction reached the seventh cornice. At this stage the inclination was about 0.6˚ and during the next 90 years increased to about 1.6˚. After the completion of the bell chamber, the inclination increased significantly. In 1817, according to the first recorded measurement (Cresy and Taylor) the inclination of the Tower was 4.9˚. The excavation of the catino in 1838 and the continuous pumping in order to prevent it from consequent water inflow caused an increase in the inclination of about 0.5˚. In 1990 the inclination of the Tower was 5.5˚.

We should notice that when a definite value of the height of the building had been reached, there was an abrupt increase in the inclination. This is a clear sign of an impending phenomenon of instability of equilibrium which is known as leaning instability and will be discussed later in this chapter.

1.3 SUPERSTRUCTURE PROFILE

The Tower of Pisa is in the form of a hollow cylinder and is made up of the foundations and the elevation, while in the middle there is the marble catino. The building is 58 m high and the foundation is 19.6 m in diameter. The elevation is externally divided into eight levels (the base, six ringed galleries and the bell chamber) and internally formed of two tubular walls which enclose the long, winding staircase that leads to the loggias. The Tower has also two shorter winding staircases, leading to the bell chamber and the terrace, and six bronze bells (the Dal Ponzo one has been removed since 2002). Each order is ornamented with columns, plinths and capitals. The base is decorated with three reliefs arranged on the sides of entrance. The cross-section of the Pisa Tower is depicted in figure 1.5.

The weight of the Tower is approximately 142 MN and the average foundation pressure is 500 kPa. A computer analysis indicates that the pressure at the south edge is about 1000 kPa, while the pressure at the north edge is close to zero as expected since the Tower is close to toppling over. The height of the center of gravity is equal to 22.6 m and its horizontal movement, which corresponds to the southward rotation of the building of about 5.5°, is approximately equal to 2.3m. The overturning moment applied on the building due to the eccentricity of its center of gravity is equal to 327 MNm. It should be noted that the rotation of the Tower except for threatening its safety due to a possible failure of its foundation, has unfavorable effects on the masonry strength of the monument too, especially when combined with some particularly critical details. A structural survey allowed a “critical zone” to be identified at the first loggia: the helicoidal stairs and the door that opens onto the loggia considerably reduce the resisting cross-section of the building. Moreover, the external marble facing at the level of the loggia is interrupted and presses onto the scarce quality conglomerate underneath with a very high compressive stress. A number of cracks and damaged zones, signs of excessive local compression

and of decreased strength, were also discovered. A detail of the cross-section of the building in the area of “critical zone” is shown in figure 1.6.

The masonry cylinder is a typical example of the so called “infill masonry” structure composed of internal and external facings and of a rubble infill cemented with mortar as illustrated in figure 1.7. A detailed survey was carried out together with chemical, mineralogical, petrographic and physical studies in order to gain knowledge of the constitutive materials of the building. San Giuliano marble is the most abundant original stone in the Tower, constituting almost all the structural parts and architectural elements. Filettole dark-grey limestone was used to form the dark ornamental bands of the façade. Apuanian marble varieties were used to substitute in different periods both San Giuliano marble and Filettole dark-grey limestone. Other materials that have been recognized are Agnano and Caprona breccias, “Panchina” calcarenite, Granodiorite, Crespignano quartzite, “Macigno” sandstone and “Lavagna” slate. The infill material of the cylinder structure and foundations is composed of fragments of the same lithotypes that make up the facing walls and of gravel and sand, all of which have been cemented with lime-mortar. The volume ratio of mortar/rubble elements is roughly uniform throughout the masonry body: the mortar content is about 1/3 by volume. The mortar composition varies according to the level and stage of construction, and even within each single level. The stones mostly come from the nearby quarries of the Monti Pisani and Monti d’Oltre Serchio areas and were brought to Pisa along various waterways: the Arno river from the from the mountains or from the sea and the Serchio river from the north.

1.4 SYNOPSIS OF THE GEOTECHNICAL STABILISATION MEASURES

The International Committee, apart from the structural strengthening and the restoration of the monument surfaces, was entrusted with the geotechnical stabilization of the Tower, a task that would obviously take a great deal of time. As a result, the Committee took an early decision to implement short term temporary measures to slightly increase the stability and to gain time to complete the study of the final stabilization. Since the temporary measures could not fully satisfy the requirements of restoration, it was essential that they should be completely reversible. The observation that the northern side of the foundations had been steadily rising led to the

suggestion that the application of a load to the foundation masonry on the north side could reduce the overturning moment. Accordingly, a design was developed that consisted of a post-tensioned concrete ring cast around the base of the Tower to support a number of lead ingots. The placement of lead ingots is shown in figure 1.8. Of course, before the implementation of this solution, both plain strain and three dimensional analyses were carried out which, combined with the observed movements due to the counterweight, led to a final refined model in order to avoid an unexpected response of the Tower. A total 6.9 MN of ingots were installed between May 1993 and February 1994. On February the northward change of inclination was 33". By the end of July it had increased to 48". On the whole, the overturning moment was reduced by 14% and the Tower experienced a northwards rotation of 52.6" and a small settlement equal to 3.3 mm. The settlement and rotation produced by the counterweight had been predicted by the finite element analysis, increasing confidence in the model. Above all, the fact that the progressive southward inclination of the Tower had come to a standstill was very satisfactory.

Soon after the application of the counterweight, various situations led to the development of another medium term temporary intervention for the safeguarding of the Tower. This was the ten-anchor solution which suggested the replacement of the lead ingots with ten tensioned cables anchored in the lower sands at a depth of over 40 m. The advantages of this measure were both the invisibility of the anchors and a slightly larger stabilizing moment due to the increased lever arm. The ten anchors had to be connected to the Tower base through a post-tensioned concrete ring beam, placed beneath the marble walkway floor and thus involving delicate excavations around the Tower and below the water table. It was decided to employ local ground freezing immediately below the catino, but above the foundation level. In addition, the post-tensioned concrete ring was to be installed in short sections so as to limit the length of excavation open at any time. Freezing and excavation were successfully carried out on the north side but, when progressing southward, the Tower began to rotate southward at about 4 arc seconds per day. After an attempt at controlling the rotation with more lead ingots, the operation was stopped and the solution was abandoned.

Concerning the conception and design of the permanent stabilization measures, the analysis of leaning instability, taking into account the nonlinear and non-elastic restraint exerted by the

ground-foundation system, was of great importance. It led to the idea that a decrease in the inclination of the Tower would greatly increase the rotational stiffness of the system and hence safety against leaning instability. The Committee concluded that a decrease in the inclination of the building by half a degree would have been sufficient to stop the progressive tilting. The decrease had to be obtained by including a differential settlement of the Tower to oppose the existing one, by acting on the foundation. Three possible solutions were extensively studied by the Committee: the construction of a slab pressing on the ground to the north of the Tower, the consolidation of the Pancone clay north of the Tower through electro-osmosis and, finally, the controlled removal of small volumes of soil beneath the north side of the foundations.

After intense investigations both the electro-osmosis and the pressing slab solution were rejected and the measure of underexcavation was adopted. However, since the Tower was very close to leaning instability, a large number of experiments and analyses was carried out before the implementation of the solution. Small-scale model tests carried out at natural gravity and in centrifuge and numerical analyses gave a favorable response, encouraging the Committee to undertake a large-scale experiment, to develop the field equipment and explore the operational procedures. A 7 m diameter eccentrically loaded instrumented footing was constructed in the Piazza north of the Baptistery for this purpose and subjected to underexcavation as shown in figure 1.9. The trial was very successful. It should be reported that all the above mentioned investigations indicated the occurrence of a critical line beyond which ground removal would aggravate inclination, instead of reducing it.

The next step was to perform a preliminary and limited ground extraction beneath the Tower itself, to observe its response. The process used for soil extraction is depicted in figure 1.10. To prevent any unexpected averse movement of the monument, a safeguarding structure was necessary. This structure consisted of two sub-horizontal steel stays, connected to the Tower at the level of the third order, and to two anchoring frames located some 100 m apart and its purpose was to apply a stabilizing moment to the Tower only if needed. The preliminary underexcavation carried out operating with 12 inclined drill holes and a total of 7 m^3 of soil was removed. The Tower rotated northward by 130".

After the very positive results of the preliminary underexcavation, the Committee continued steadily with the full underexcavation as presented in figure 1.11. A total of 41 holes were bored and a total of 38 m^3 of soil was removed. All the lead ingots and the ring beam were removed in the same period. The steel cable stays were also dismantled in June 2001. The goal of decreasing the inclination of the Tower by half a degree had been achieved. The settlement on the north side of the foundations was over 160 mm, while on the south side there was a heave of 11 mm.

1.5 INSTABILITY OF EQUILIBRIUM

A detailed history of the inclination of the Tower, and in particular, of the movements it has experienced in the last century has been developed thanks to a very comprehensive monitoring system, installed on the Tower since the beginning of the 20th century and progressively enriched. The behavior of the Tower clearly indicates that it is affected by leaning instability, a phenomenon controlled by the stiffness of the soil rather than by its strength (Gorbunov Possadov and Serebriany, 1961; Habib and Puyo, 1970; Schultze, 1973; Hambly, 1985; Lancellotta, 1993; Desideri and Viggiani, 1994; Desideri et al., 1997; Potts and Burland, 2000; Jamiolkowski et al., 2000).

In order to demonstrate leaning instability, a simple conceptual model of an inverted pendulum can be used as shown in figure 1.12. The model consists of a rigid vertical pole with a concentrated mass at the top which is hinged at the base to a constraint that reacts to a rotation with a stabilizing moment. The rotation induces an offset of the mass and, as a result, an overturning moment. In the vertical position, the system is in equilibrium. If a rotation occurs, there are three possible ways for the system to respond. If the stabilizing moment is larger than the overturning one, the equilibrium is stable and the system returns to the vertical configuration. If the contrary occurs, the equilibrium is unstable and consequently the system collapses. If the two moments are equal, the equilibrium is neutral and the system stays in the displaced configuration. The above mentioned states of equilibrium are schematically described in figure 1.13. As far as tall structures are concerned, there is a significant possibility that either an eccentricity of the center of gravity of the building on its base or an initial inclination developed during construction will generate an overturning moment. Consequently, sufficient measures should be implemented in order to avoid leaning instability.

Modeling the Tower as inverted pendulum and the foundation as a circular plate of diameter D resting on an elastic half space of constants E, v (Desideri and Viggiani, 1994, Desideri et al., 1997), the restraint exerted by the foundation may be evaluated. An overturning moment M_o is applied on the Tower, due to its inclination, which is equal to $M_0 = W \cdot h_c \cdot \sin\theta = W \cdot h_c \cdot \theta$ ($\sin\theta = \theta$ for small angles), wherein W is the weight, h_c is the height of the center of gravity above the foundation and θ is equal to the rotation of the Tower measured in rad. The rotation of the building generates a resisting moment M_r, thanks to the reaction of the foundation soil, which is equal to $M_r = K_R \cdot \theta$, wherein $K_R = \frac{E \cdot D^3}{6(1-v^2)}$ is the rotational stiffness of the soil underneath the Tower. An evaluation of the safety factor FS may be obtained by the knowledge of the settlement of the Tower that is around 3 m and gives $\frac{E}{(1-v^2)} = 2.85 \mathrm{MN/m^2}$. Consequently, we estimate FS as follows:

$$FS = \frac{M_r}{M_o} = \frac{K_R \cdot \theta}{W \cdot h_c \cdot \sin\theta} = \frac{K_R}{W \cdot h_c} = \frac{E}{6 \cdot \left(1 - v^2\right)} \frac{D^3}{W \cdot h_c} = 1.12$$

It is obvious that the Tower is very near a situation of neutral equilibrium. It should be noted though that the relationship between Mr and θ may be linearized over a short interval, but it is certainly non-linear and approaches a limiting value of Mr asymptotically. Especially in the case of Pisa Tower, which is on the verge of leaning instability, consideration of non-linearity is essential. To this aim, the knowledge of the relationship $M_r = M_r(\theta)$ and in general the choice of an appropriate constitutive model for the subsoil is necessary.

FIGURES OF CHAPTER 1

Figure 1.1 Piazza dei Miracoli

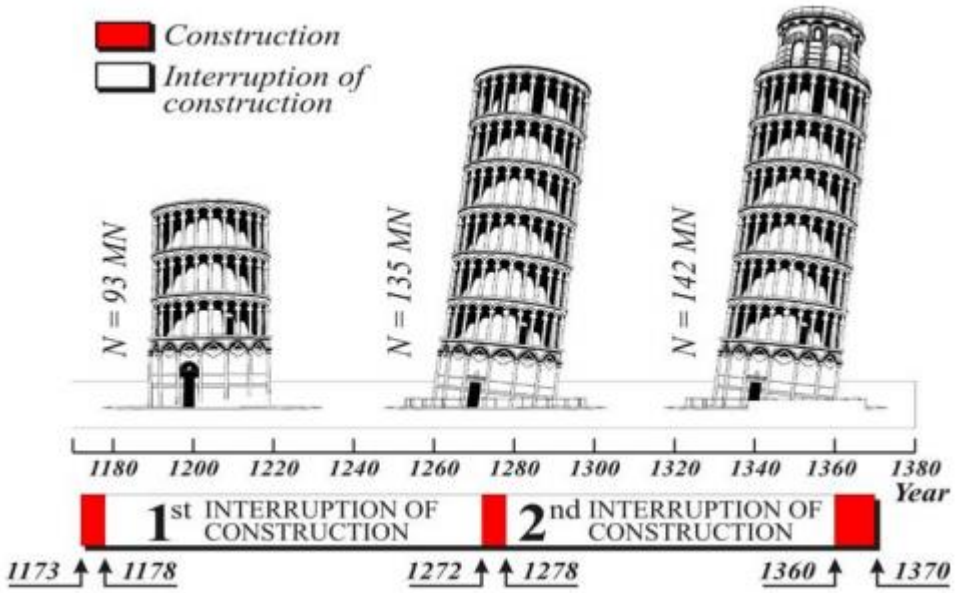

Figure 1.2 History of the construction

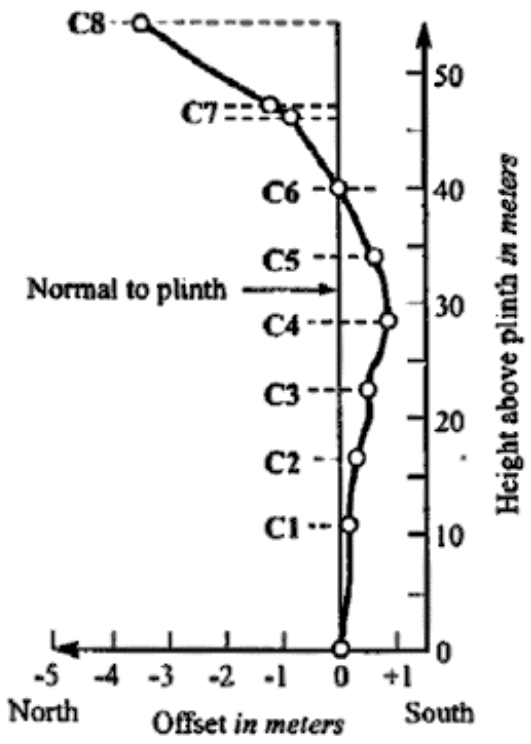

Figure 1.3 Shape of the axis of the Tower

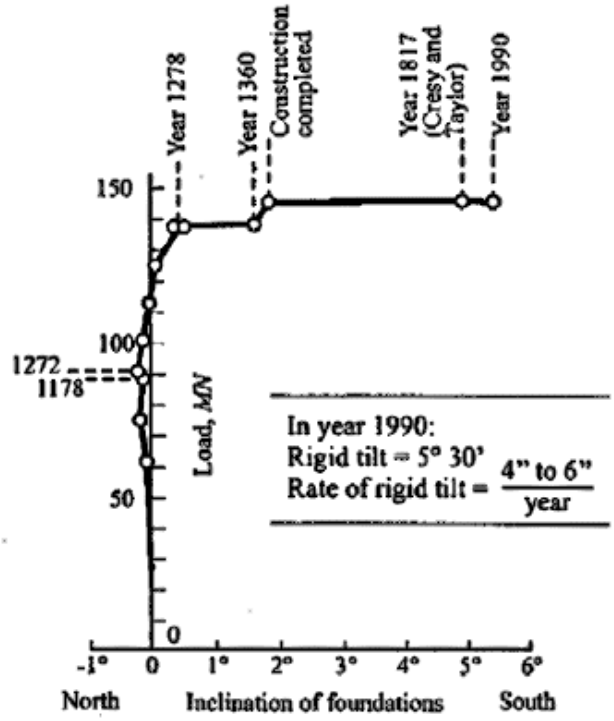

Figure 1.4 History of inclination

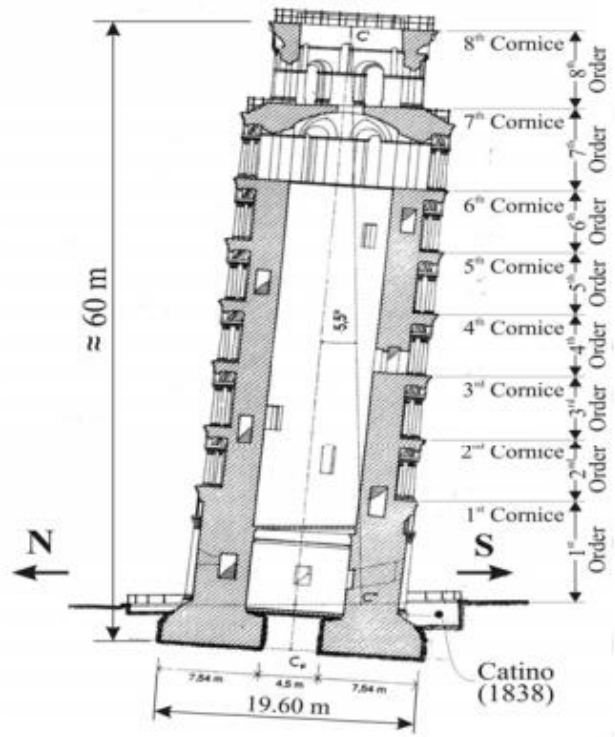

Figure 1.5 Cross-section of the Tower of Pisa

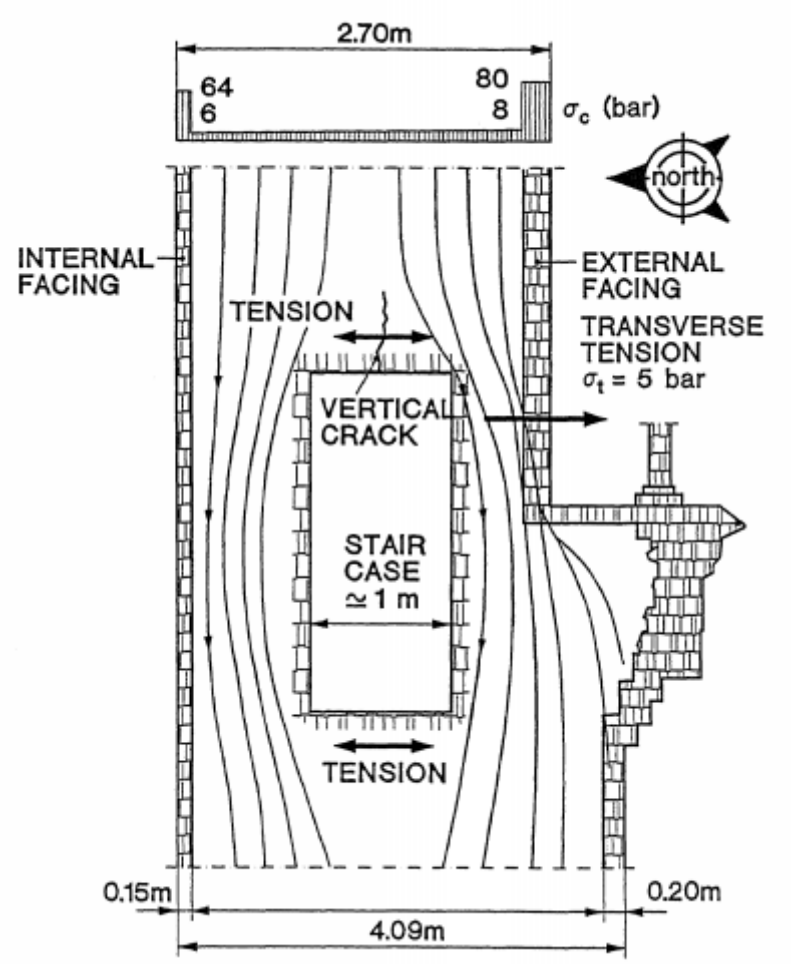

Figure 1.6 Critical zone of the first cornice

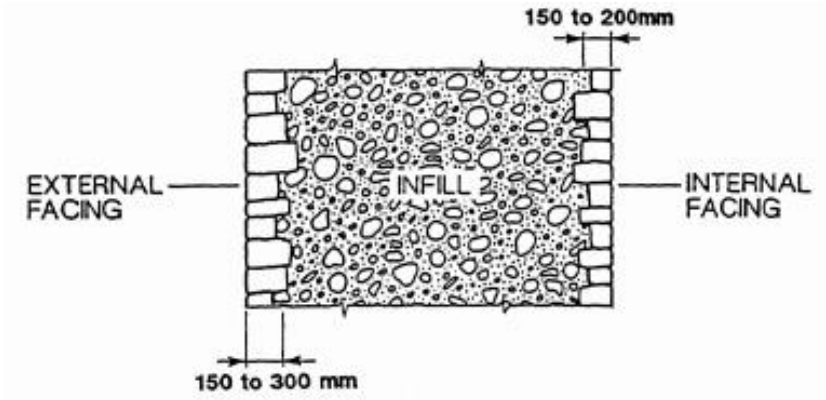

Figure 1.7 Cross-section of masonry

Figure 1.8 Lead counterweight on the North Side

Figure 1.9 Large scale experiment

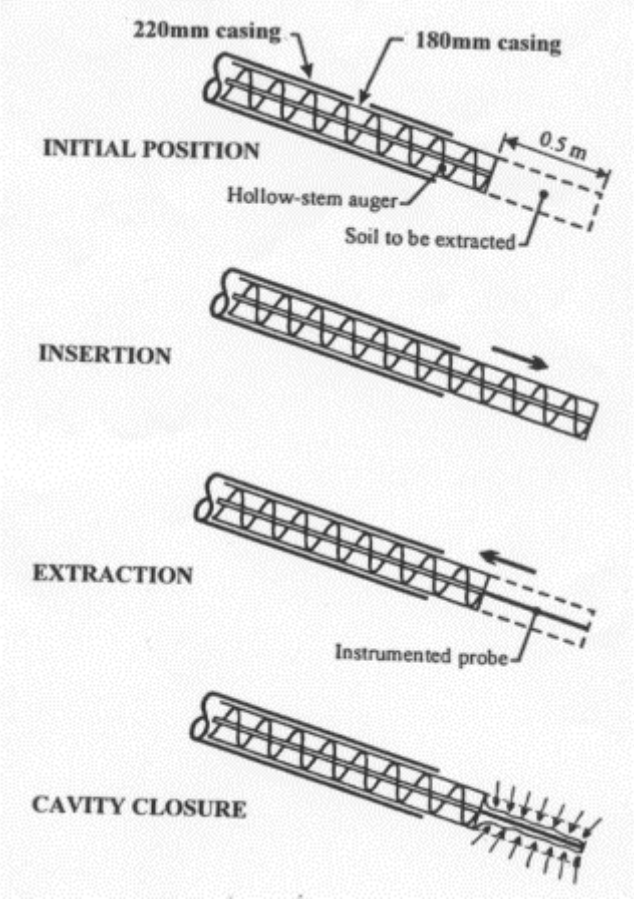

Figure 1.10 Drilling technique adopted to remove the soil

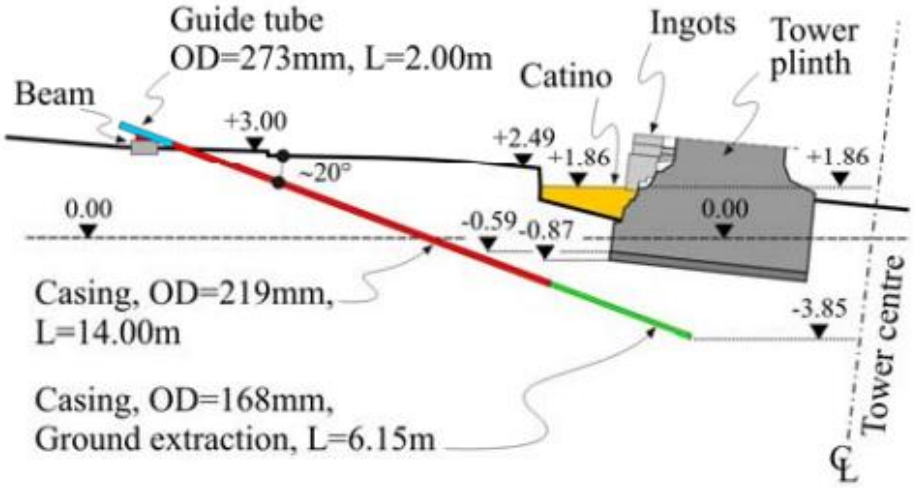

Figure 1.11 Extraction hole of massive underexcavation

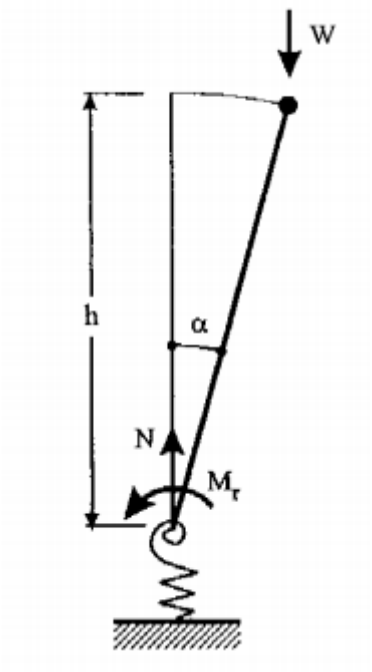

Figure 1.12 Inverted pendulum model

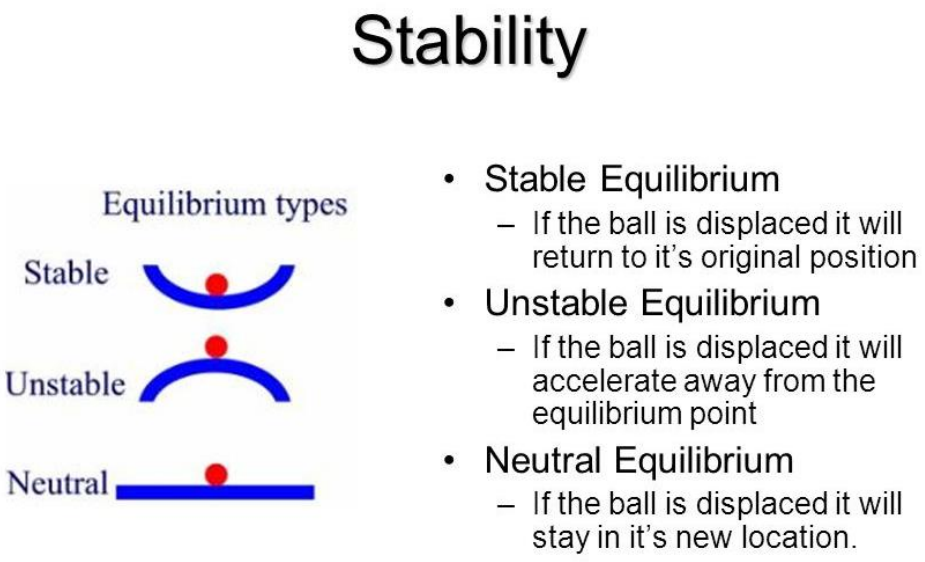

Figure 1.13 States of equilibrium

CHAPTER 2
GEOTECHNICAL CHARACTERIZATION OF PISA SUBSOIL

2.1. INTRODUCTION

Since the beginning of last century, 16 Committees have been appointed to undertake studies aimed at the stabilization of the leaning Tower of Pisa. During that period, a large number of laboratory and in-situ tests were carried out, providing a huge amount of information about the subsoil profile and its physical and mechanical properties. Extensive investigations that were performed included in situ CPT and boreholes with both Kjellman, Denison and mechanical piston sampling (Polvani Committee) and CPT, CPTU and boreholes with mechanical piston sampling (Project Team led by Finzi and Sanpaolesi). The provided information from the above mentioned investigations were thoroughly studied and enriched by the International Committee that carried out boreholes with piston, Laval and Begemann sampling, Seismic Cone Penetration Tests, Cross-Hole Tests, Seismic Analysis of Surface Waves (SASW) tests, as well as additional CPT and CPTU tests. In this chapter, we summarize and present the characterization of the subsoil profile of the Tower and its geotechnical properties some of which are essential for the following analyses.

Another topic that is of great importance, in order to better comprehend the behavior of the leaning Tower and its subsoil, has to do with the proper simulation of the problem and the analysis procedure that will be selected. Both small scale tests and finite element analyses were carried out, so as to simulate the rotation of the building, point out the dominant failure mechanisms of the structure-subsoil system and eventually predict the response of the Tower to the designed stabilization measures. Some of the most important models will be discussed herein.

2.2. SUBSOIL PROFILE AND GROUNDWATER CONDITIONS

The Piazza dei Miracoli is constructed on the alluvial sediments that infilled the lower Arno River valley, which was excavated during the glacial periods, at a level of only 3-4 m above the mean sea level. The subsoil profile consists of three distinct horizons:

1) Horizon A: upper variable deposits from 3 to 10 m

2) Horizon B: clayey deposits from 10 to 40 m

3) Horizon C: lower sand deposits from 40 to 60 m.

Moreover, a heterogeneous silty-clayey soil, containing archaeological remains, has been identified from ground level to a depth of about 3 m. The subsoil profile and the sublayers of each stratum as described next are depicted in figures 2.1 and2.2 respectively.

Horizon A is about 10 m thick and consists above all of estuarine deposits, laid down under tidal conditions. Consequently, the deposits mainly contain sandy and clayey silts of various thickness and differ considerably over short horizontal distances. The deposition environment also explains the observation of inclined layers having variable dip direction. Based on sample descriptions and piezocone tests, the materials to the south of the Tower appear to be more silty and clayey than to the north, and the sand layer is locally thinner. On the whole, the cone resistance qc yielded by CPTUs reveals that the resistance of horizon A is lower to the South when compared to that of the North side. At the bottom of Horizon A there is a 2 m thick medium dense fine sand layer.

Horizon B is about 30 m thick and consists primarily of marine clay. It is subdivided into four distinct layers. The “upper clay”, known as Pancone, is a soft sensitive deposit of high plasticity that loses strength when disturbed. Under this a 4 m layer of stiffer clay can be found, the “intermediate clay”, which, in turn, rests upon a 2 m thick layer of “intermediate sand”. Both strata are similar to the deposits of Horizon A, since deposited in an estuarine environment. The bottom layer is a normally consolidated soft clay known as the “lower clay”.

Horizon C would have been the initial fill of the valley and consists of dense marine sands, known as the “lower sand”, which extends to a considerable depth.

The phreatic surface is found at the elevation of approximately 1.8 m above sea level. Pumping from the “lower sand” in the larger area of Pisa lead to a reduction of the hydraulic head in Horizon C with a pore pressure distribution to depth slightly below hydrostatic.

The kinematics of the displacements of the foundations led to the conclusion that the continuously long term tilting of the Tower can be put down to Horizon A and not to the underlying Pancone clay, as had widely been assumed in the past. It is remarkable that the Tower does not tilt in the east-west direction. Finally, the many borings beneath and around the Tower showed that the surface of the Pancone clay is dished beneath the Tower and the average settlement of the monument was measured to be approximately 3 m.

2.3. PHYSICAL AND INDEX PROPERTIES

Mean values of the main physical and index properties of each sublayer are reported in Table 1. To be more specific, unit weight γ, specific gravity G, natural water content w_N, liquid limit w_L, plasticity index I_p and liquidity index LI are presented.

The cohesive part of Horizon A is a clayey silt of low plasticity, with the natural water content about 25-35%, liquid limit w_L in the order of 30-40% and the plasticity index I_p about 10-20%. The “upper clay” is a grey-blue silty clay of high plasticity (w_N=50-65%, w_L=60-85%, I_p=35-55%), except for the B2 stratum which shows a lower plasticity, probably because of a temporary gradual change in the deposition conditions of the Pancone clay deposit. The “intermediate clay” is a brownish stiff silty clay, with higher unit weight, lower water content and lower plasticity than the “upper clay”. To be more specific, the plasticity index I_p is in the range of 18 to 30% and the natural water content w_N is almost equal to the plastic limit. The properties of this clay may be attributed to an emersion stage that caused some overconsolidation. The “lower clay” is a medium plasticity clay with a considerable dispersion of physical and index properties values.

As far as liquidity index LI is concerned, mean values in order of 0.5-0.7 can be attributed to the “upper clay” and the sublayers B7, B8 of the “lower clay”, whereas a smaller LI equal to about 0.1-0.3 can be attributed to the “intermediate clay” and sublayers B9, B10 of the “lower clay”.

Consequently, Pancone clay and the upper part of “lower clay” are less cohesive soils than the “intermediate clay” and sublayers B9, B10.

2.4. MECHANICAL PROPERTIES

2.4.1. Overconsolidation Ratio

Figure 2.3(a) shows the profile of the overconsolidation ratio $OCR=\sigma'_p/\sigma'_{v0}$. The preconsolidation pressure σ'_p was obtained using Casagrande’s procedure to interpret data from oedometer tests, while the in situ vertical effective stress σ'_{v0} was calculated using the unit weight and the profile of the pore-water pressure proposed by the Polvani Committee. The profiles of σ'_p and σ'_{v0} are reported in figure 2.3(b).

As far as Horizon A and “intermediate” clay are concerned, higher values of OCR are observed, probably because the deposition of these layers in an estuarine environment, where relevant phenomena of erosion and re-deposition are possible and phenomena of water table oscillation and desiccation can play a major role. Values of the overconsolidation ratio up to 4 and 3 can be attributed to Horizon A and “intermediate” clay respectively. On the contrary, marine clays, that is upper and lower clays, show lower values of OCR. More specifically, in the “upper clay” OCR ranges from 1.5 to 2, whereas values only slightly higher than unity are detected in the “lower” clay.

2.4.2. Compressibility

In order to assess the parameters of compressibility of the subsoil, oedometer tests were performed on samples retrieved with several different methods such as Osterberg samples, mechanical piston samples and Laval samples that correspond to different campaigns of investigations. Laval sampling technique was used by the International Committee and lead to more detailed and reliable results for the behavior of the subsoil under compression, since it causes little disturbance of the soil structure even to rather sensitive clays and provide samples of better quality.

Figures 2.4(a)-2.4(d) illustrate the oedometer compression curves plotted in the normalized plane I_v-logσ'_v, where I_v is the void index (Burland 1990): $I_v = \frac{e-e^*_{100}}{C^*_c}$, where: e^*_{100} is the void ratio at σ'_v=100 kPa and C^*_c is the compression index, both related to the reconstituted soil. The quantities e^*_{100} and C^*_c are considered to be the "intrinsic" parameters of the soil, because they are supposed to be independent of structural features. Since tests on reconstituted samples were not available for most of the soils described herein, the intrinsic parameters were determined using the empirical equations relating e^*_{100} and C^*_c to the void ratio at the liquid limit e_L (Burland 1990). The sedimentation compression line (SCL) and the intrinsic compression line (ICL) as defined by Burland (1990) are also plotted in the figures. The SCL is the locus of the in situ conditions for most natural normally consolidated clays, while the ICL is the normalized oedometer compression line for nearly all the reconstituted clays.

Comparison between the normalized compression lines of the subsoil layers and the SCL, ICL lines, contributes to the assessment of their microstructure and consequently, their sensitivity and compression behavior. To be more specific, as far as layer A1 is concerned, in situ states for the Laval samples lie on or above the SCL and the corresponding normalized compression curves are only slightly steeper than the SCL, and do not appear to converge on the ICL in the investigated stress range, indicating a steady open bonded structure. In situ conditions for the Laval samples of the "upper clay" lie generally well above the SCL and all the normalized compression curves of these samples cross the SCL and tend to converge on the ICL as the vertical effective stress increases. According to Burland (1990) this behavior suggests that the loads applied in the oedometer tests cause significant changes in the microstructure of the soil which progressively passes from a sedimentary state towards a reconstituted state, when the effective vertical stress exceeds the pre-consolidation stress. On the whole, the open microstructure and sensitivity of Pancone clay were confirmed thanks to the little sampling disturbance of Laval samples. Finally, the in situ data points referring to Laval samples from the "intermediate" and "lower" clays plot close or below the ICL, suggesting that the natural microstructure is similar to that of the reconstituted soil. The normalized compression curves plot close to the ICL, as the yield stress is reached, indicating a more stable microstructure in the range of the applied stresses.

The compression and swelling indexes of each stratum are shown in figure 2.5. In the case of Pancone clay, the oedometer virgin compression curves of the Laval samples are not straight, indicating higher compressibility of the soil immediately after the yield stress than the compressibility at much higher stresses. Thus two values of C_c were determined: C_{c1} for the initial slope and C_{c2} for the second one. Moreover, two values of the swelling indexes were computed: C_{s1} that corresponds to the first unloading step and C_{s2} that corresponds to the last unloading step.

2.4.3. Undrained Shear Strength

The in situ shear strength of clay layers of the subsoil was determined from standard K_0-consolidated undrained triaxial compression tests and K_0-consolidated undrained direct simple shear tests and the values obtained are shown in figure 2.6. In layer A1, S_u ranges from 50 to 75 kPa. In the Pancone and "lower" clay, except for stratum B9, a single linear relationship between the undrained shear strength and the elevation could be inferred, with values of S_u in the range of 30 to 75 kPa. In the Intermediate Clay and in sublayer B9, higher values are detected that are about 80 to 140 kPa and 100 to 120 kPa respectively.

2.4.4. Soil Stiffness

The stiffness of Pisa subsoil from small to very large strains was thoroughly examined by performing several kind of laboratory tests including Resonant Column Tests on isotropically consolidated specimens, drained monotonic loading torsional shear tests on isotropically and K_0-consolidated specimens, drained and undrained compression loading triaxial tests on isotropically and K_0-consolidated specimens. The small strain shear modulus G_0 was also determined by means of in situ tests carried out, so as to define the profile of shear wave velocity Vs, since it can be expressed as $G_0 = \rho \cdot V_s^2$. In situ seismic methods included Crosshole, Downhole and SASW tests. The obtained results were very consistent with the exception of the first meters where Downhole tests underestimated the shear wave velocity as shown in figure 2.7.

In order to separate the influence of effective confining stresses from that associated with soil structure on small strain shear modulus G_0, the following empirical equation has been used

(Jamiolkowski et al. 1995): $G_{vh}=C_{vh}\cdot e^{-x}\cdot \sigma_v^{'n}\cdot \sigma_h^{'n}\cdot p_a^{1-2n}$. Meanwhile, the referring to the upper Pancone clay values of G_0, as defined by laboratory tests, were normalized by the void ratio function $F(e)=e^{-1.43}$ (Jamiolkowski et al. 1995) and plotted in figure 2.8 together with the best fit line. All the data are close to the best fit line and clearly indicate that G_0 is only moderately influenced by the strain rate, while it is independent of OCR, after a normalization by an appropriate void ratio function. The latter can be explained, considering that, for a given soil, the current void ratio, stress state and OCR are linked to each other and consequently, for a given stress state only one parameter in necessary to express the soil state. It is thus possible for an expression similar to the one mentioned at the beginning of this paragraph to represent the small strain stiffness. Processing of the laboratory results for Pancone clay led to a calibrated form of the small strain shear modulus as follows: $G_{vh}=480\cdot e^{-1.43}\cdot \sigma_v^{'0.22}\cdot \sigma_h^{'0.22}\cdot p_a^{0.56}$. Despite the fact that the database used to obtain such an equation refers to the upper Pancone clay, it is also used to predict the initial stiffness in all the layers of Pisa subsoil. The profiles of small strain shear modulus as obtained by means of both laboratory and in situ tests as well as the one calculated by the above mentioned equation are illustrated in figure 2.9, where we can observe the good agreement between the results.

2.5. SIMULATIONS IN LITERATURE

Edmunds (1993): A number of small scale physical tests was performed by Edmunds, to study the effect of underexcavation on a Tower close to collapse for leaning instability. The model used, which is depicted in figure 2.10(b), consisted of a Tower with a diameter of 102 mm which was placed on top of a very loose fine sand bed and loaded through a hanger at a height of 126 mm over the base. The ratio 126/102 is approximately equal to the ratio of the height of the center of gravity of the Tower of Pisa to the diameter of its foundation (22.6/20).

Loading the model Tower resulted in a settlement and a rotation α. A total of 8 load tests were carried out. The load at failure varied between 120 and 190 N. In all cases, failure was by toppling with the lowest edge of the model tower's base sinking into the sand as the Tower rotated toward horizontal. The individual plots of α varying with load give somewhat variable results, but when

combined into one plot, as shown in figure 2.10(a), a well-defined envelope of results emerges. The envelope clearly shows a change in curvature at a load of 160 to 165 N, where the slope of the Tower averages 0.09 ($\alpha \approx 5°$).

After this preliminary investigation, a total of 14 underexcavation tests were performed starting with a load of 165 N and a rotation of 5.5°, since these conditions were representative of a tower close to leaning instability. Underexcavation was performed by inserting a stainless steel tube and inside it an inner tube connected to a vacuum pump. The inner tube removes the sand from inside the larger tube that is thus advanced into the soil by a form of self-boring, without significant disturbance of the surrounding soil. Different combinations of probe positions and penetration sequence were performed. Important indications emerged from these tests most of which applied to the case of the Tower of Pisa. Notable is the fact that underexcavation proved to be a sufficient method to reduce the tilt of the model in a controllable manner (reduction of tilt up to 1° had been obtained), as well as the existence of a critical point north of the central axis of the Tower, in the ground beneath it, beyond which ground removal aggravates the tilt.

Potts and Burland (2000): In order to investigate the differences between leaning instability and the usual bearing capacity failure, Potts and Burland carried out Finite Element Analysis of the behavior of a simplified model of the Pisa Tower and its subsoil. The model as illustrated in figure 2.11(a) consists of a Tower resting on a uniform deposit of undrained clay which is modelled as a linear elastic- perfectly plastic Tresca material with an undrained shear strength S_u=80 kPa. The Tower was given an initial tilt of 0.5° and the self-weight was then increased in a large displacement finite element analysis. Shear stiffness G was used as a parameter and, specifically, two analyses were performed, one considering G/S_u =10 and one considering G/S_u =1000. In reality, soil properties are likely to lie between these two extreme values of shear modulus G. The weight-rotation curves obtained for each analysis are plotted in the same diagram shown in figure 2.11(b). As we can observe, failure occurs with little warning and the weight of the Tower at this point depends on the shear stiffness of the soil. To be more specific, the failure load with G/S_u =10 is about half of that with G/S_u =1000, meaning that the stiffer soil withstands greater loading. Moreover, the higher the shear stiffness of the soil is, the less the Tower rotates for a certain weight applied, due to the higher rotational stiffness of the soil.

As far as the type of failure mechanism is concerned, some interesting observations are made when comparing figures 2.12(a) and 2.12(b), that illustrate vectors of incremental displacement for the stiff and soft soil respectively, just before failure occurs. In the case of the soft soil, the displacements are located in a zone below the foundation and indicate a rotational type of failure. Even though, at first, we assume a plastic type of failure, the examination of the zone in which the soil has gone plastic indicates that it is very small and, therefore, not consistent with a plastic failure mechanism but with leaning instability. On the contrary, vectors in the case of the stiffer soil indicate a type of "general failure" mechanism, while the plastic zone is very large and, therefore, consistent with a bearing capacity type mechanism of failure.

Numerical analysis (by ICFEP): Finite element analyses of the historical movements of the Tower were performed using a finite element geotechnical computer program developed at Imperial College and known as ICFEP (Potts and Gens, 1984). The constitutive model is based on Critical State concepts and is non-linear elastic work hardening plastic with fully coupled consolidation for all of the soil layers, so as drainage of pore water in the soil skeleton is included. The analyses aimed to contribute to the better understanding of the mechanisms controlling the behavior of the Tower (Burland and Potts, 1994). At first, a plane strain problem was thoroughly examined and only later were three dimensional analyses carried out to gain more detailed knowledge.

Figure 2.13(a) shows the adopted mesh of the model which appears to be refined in the immediate vicinity of the foundation. The subsoil is divided into layers that correspond to those described in the soil exploration studies. In Horizon B the soil is assumed to be laterally homogenous, whereas in Horizon A, a tapered layer of slightly more compressible material was incorporated into the mesh, which in applied mechanics may be considered as an imperfection, in order to simulate the more clayey material beneath the south side of the foundation. The construction history of the Tower was simulated by a series of load increments applied to the foundation at suitable time intervals. The overturning moment M generated by the Tower weight W acting eccentrically at a height h_c, when any change of inclination of the Tower takes place, is given by the expression $M=W\cdot h_c\cdot\sin(\theta)\cdot I_c$, where the correction factor I_c allows for the difference between the plane strain and three dimensional conditions. Its theoretical value should be equal to 1.266, however the angle of rotation predicted was smaller than the actual one and therefore a

number of runs were carried out, so as to appropriately adjust the model. The best fit with the history of the Tower was obtained at I_c=1.27, resulting in a rotation of 5.44°. Figure 2.13(b) shows a graph of the predicted changes in inclination of the tower against time for the refined model, compared with the deduced historical values. From about 1272 onwards there is a very good agreement between the model and the historical inclination. Any further increase in I_c resulted in instability of the Tower, making clear the fact that the Tower must have been very close to falling over.

Numerical analyses were also made, in order to define the mechanisms that control the Tower behavior during the application of safeguarding measures and, specifically, Tower's response to lead ingots counterweight and soil extraction. Further adjustments were made to improve the model behavior and important observations were made, such as confirmation of the existence of the critical line detected by Edmunds.

FIGURES OF CHAPTER 2

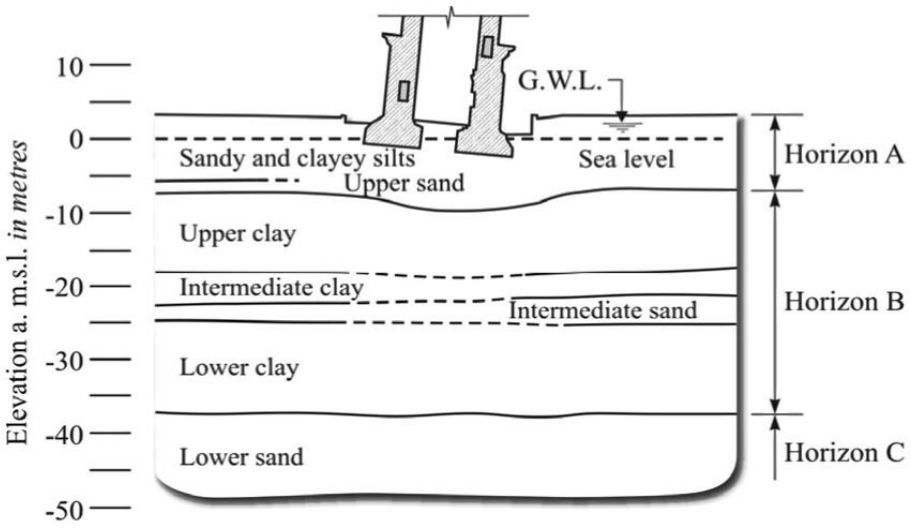

Figure 2.1 Ground profile beneath the Tower

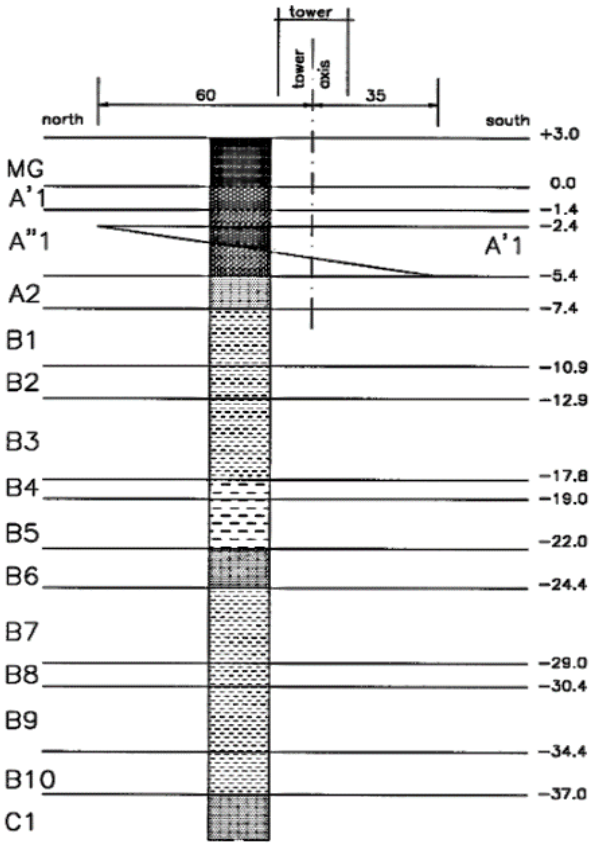

Figure 2.2 Sublayers of each Horizon

Horizon	Layer	γ kN/m^3	GS -	w_n %	w_l %	I_p %	LI -
A	A1	18.86 ± 0.72	2.71 ± 0.03	30.9 ± 4.0	35.0 ± 5.3	12.9 ± 4.1	0.68 ± 0.31
	A2	18.07 ± 0.85	2.69 ± 0.04	37.3 ± 6.6	55.7 ± 7.8	30.4 ± 7.1	0.62 ± 0.20
B	B1	17.00 ± 0.89	2.76 ± 0.04	50.7 ± 12.5	73.1 ± 9.4	42.7 ± 7.8	0.56 ± 0.29
	B2	17.49 ± 0.57	2.76 ± 0.02	46.5 ± 6.7	59.2 ± 13.6	32.7 ± 12.0	0.73 ± 0.34
	B3	16.67 ± 0.58	2.75 ± 0.04	56.3 ± 7.5	70.9 ± 14.3	41.2 ± 11.4	0.72 ± 0.52
	B4	19.48 ± 0.96	2.72 ± 0.02	27.7 ± 8.4	53.2 ± 11.9	33.3 ± 9.3	0.27 ± 0.30
	B5	19.76 ± 0.79	2.75 ± 0.03	27.4 ± 5.9	46.3 ± 10.9	22.8 ± 9.6	0.15 ± 0.19
	B6	19.11 ± 0.49	2.70 ± 0.02	29.4 ± 2.9	33.0 ± 5.7	8.5 ± 3.5	0.59 ± 0.51
	B7	18.62 ± 0.97	2.75 ± 0.03	38.5 ± 8.9	59.7 ± 18.0	33.9 ± 15.3	0.41 ± 0.13
	B8	18.41 ± 0.51	2.72 ± 0.04	37.1 ± 5.0	48.9 ± 5.3	22.6 ± 8.5	0.57 ± 0.29
	B9	19.01 ± 1.41	2.66 ± 0.08	32.5 ± 9.4	54.5 ± 8.3	31.0 ± 6.0	0.21 ± 0.16
	B10	19.38 ± 0.44	2.76 ± 0.02	31.2 ± 4.1	51.3 ± 10.7	29.0 ± 10.2	0.34 ± 0.18
C	C	20.52 ± 1.29	2.65 ± 0.05	20.6 ± 8.5	-	-	-

Table 1 Physical and index properties of main soil layers

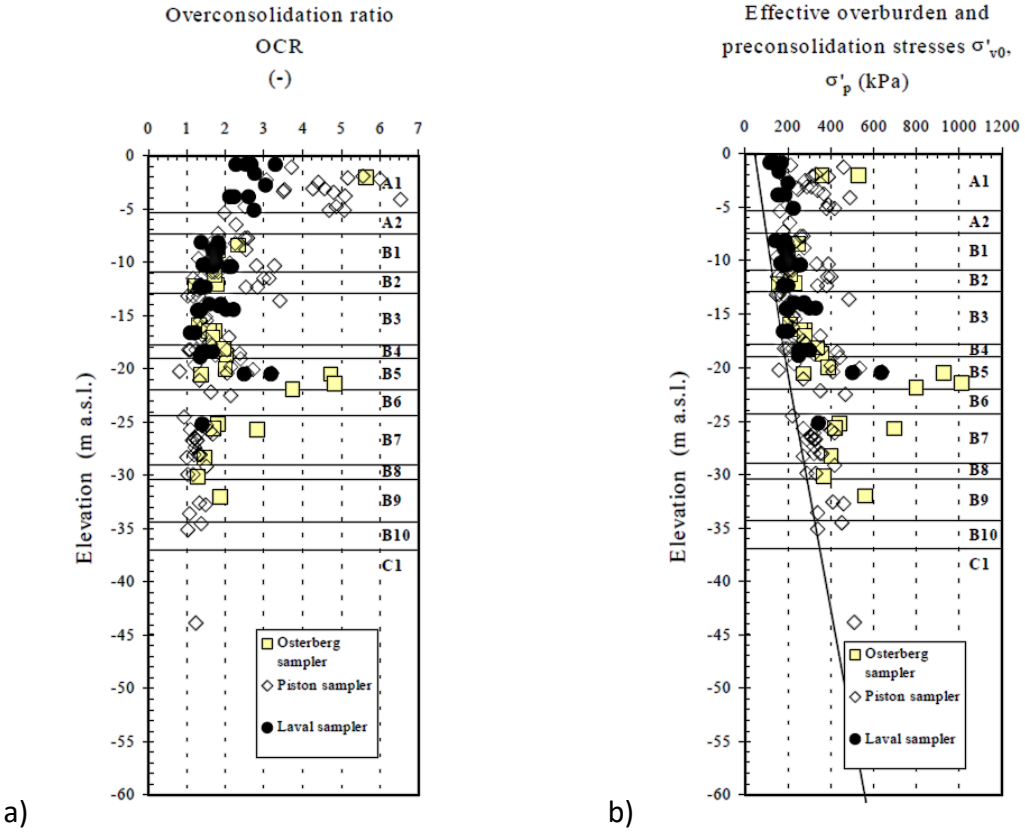

a) b)

Figure 2.3 Profiles of a) overconsolidation ratio OCR and b) preconsolidation pressure σ'_p and vertical effective stress σ'_{v0}

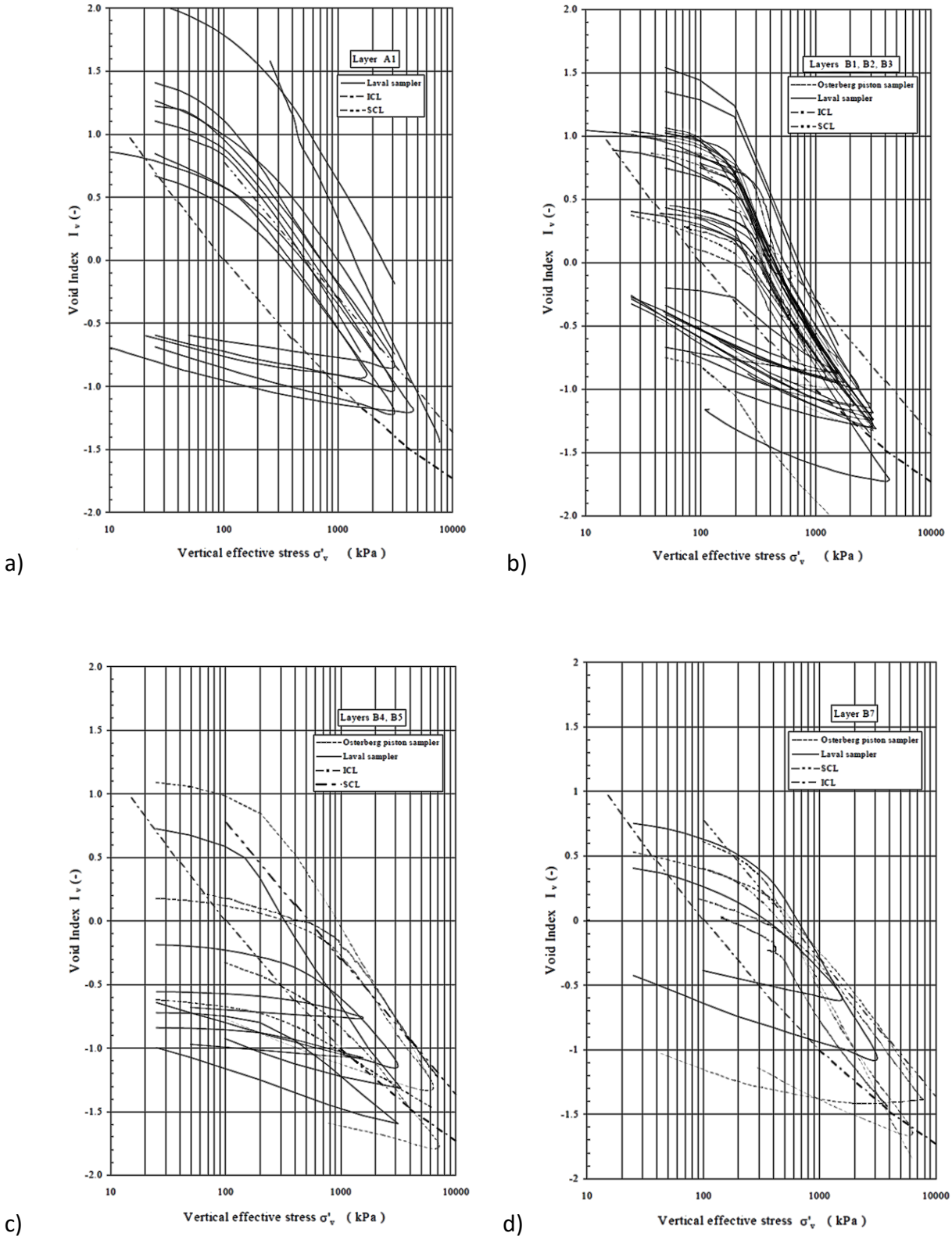

Figure 2.4 Normalized compression curves for

a) layer A1, b) Pancone clay, c) intermediate clay, d) lower clay

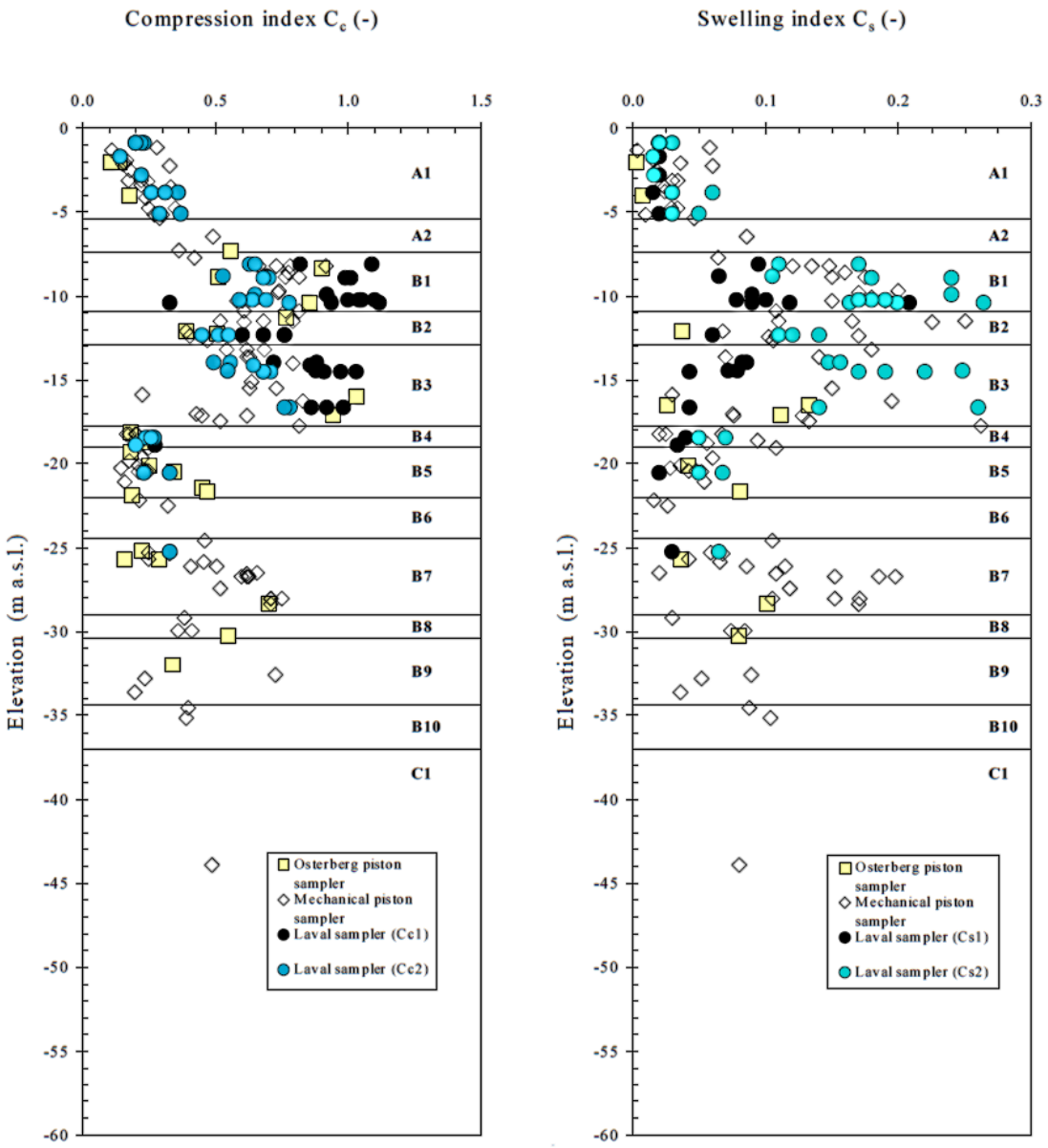

Figure 2.5 Profiles of compression and swelling indexes

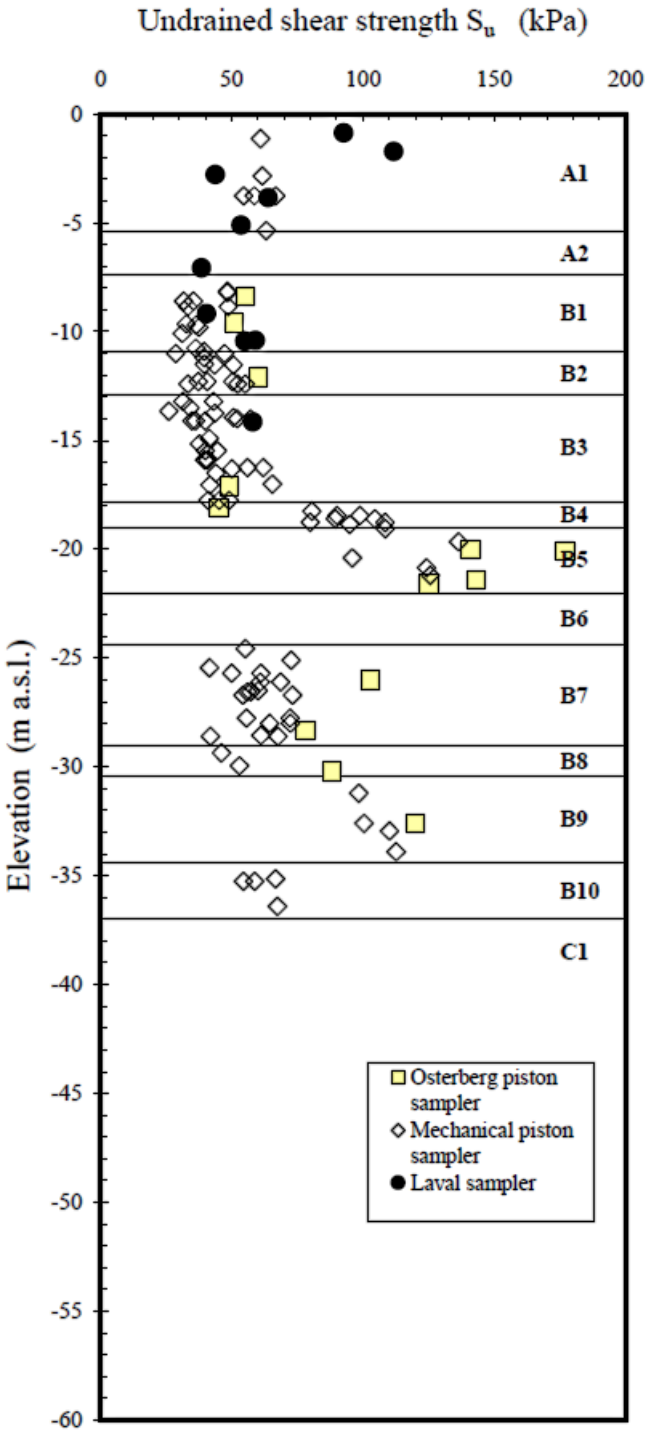

Figure 2.6 Profile of undrained shear strength

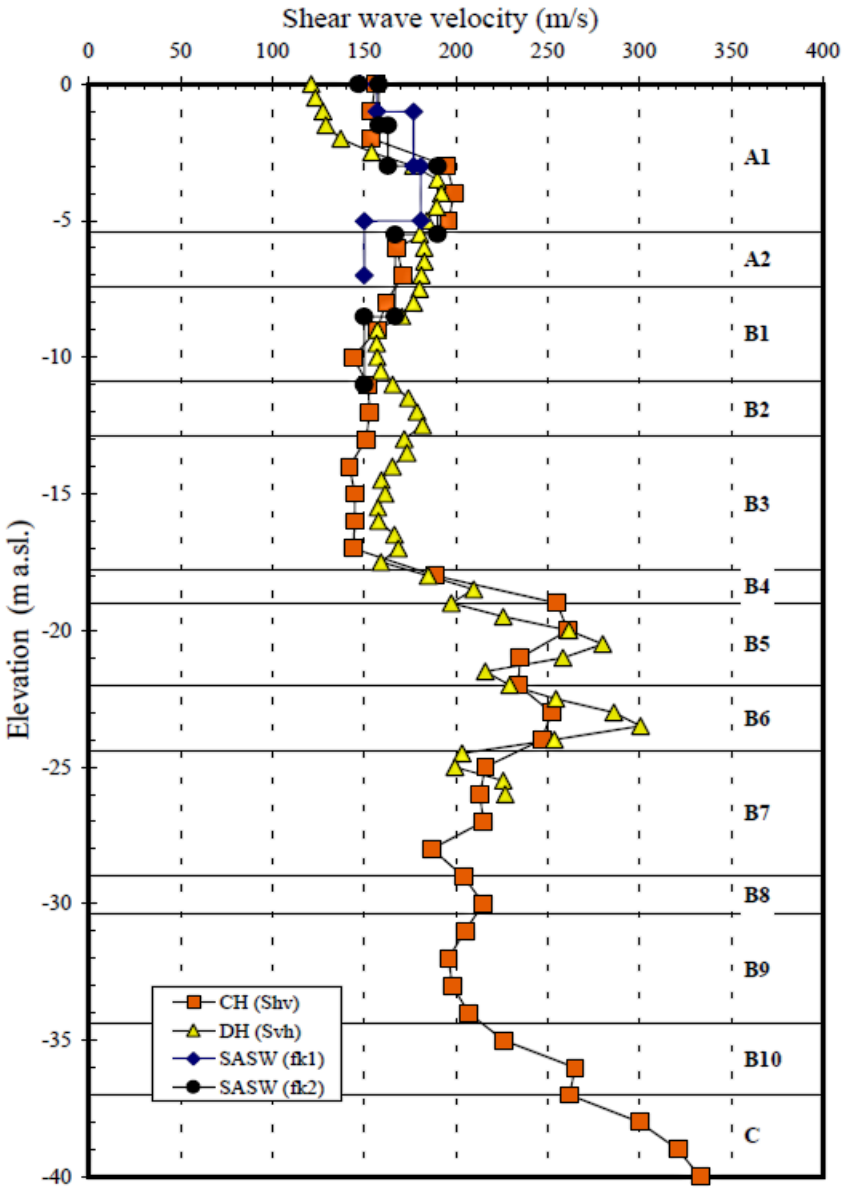

Figure 2.7 Shear wave velocity profile

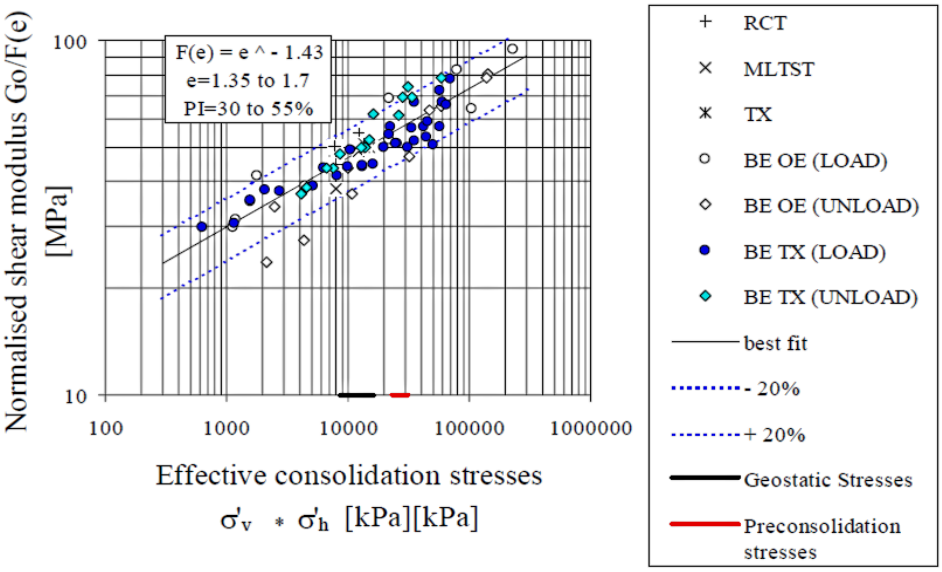

Figure 2.8 Normalized small strain shear modulus of Pisa Clay versus consolidation stress

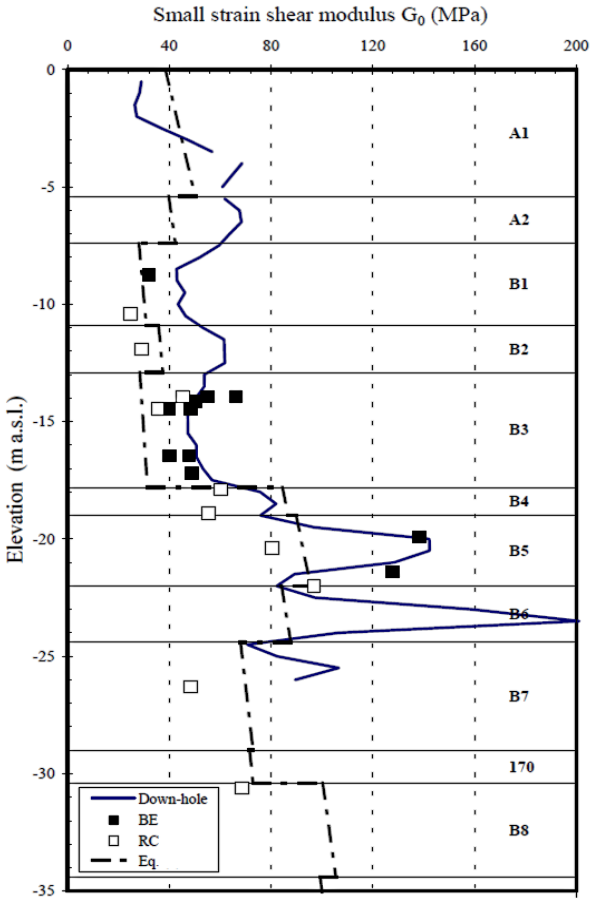

Figure 2.9 Small strain shear modulus profiles

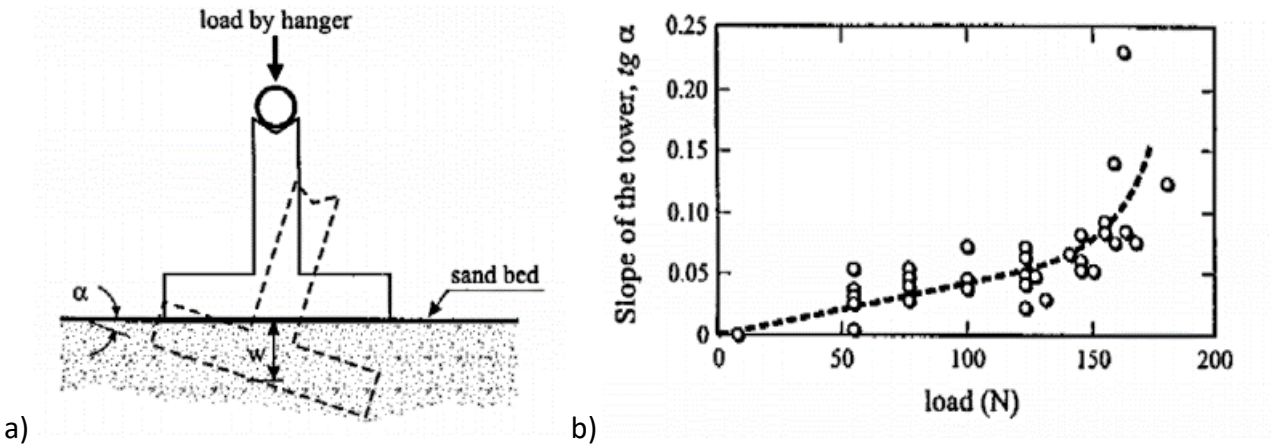

a) b)

Figure 2.10 Edmunds' small scale physical test (a) experimental set up

(b) inclination α of the model tower vs vertical applied load

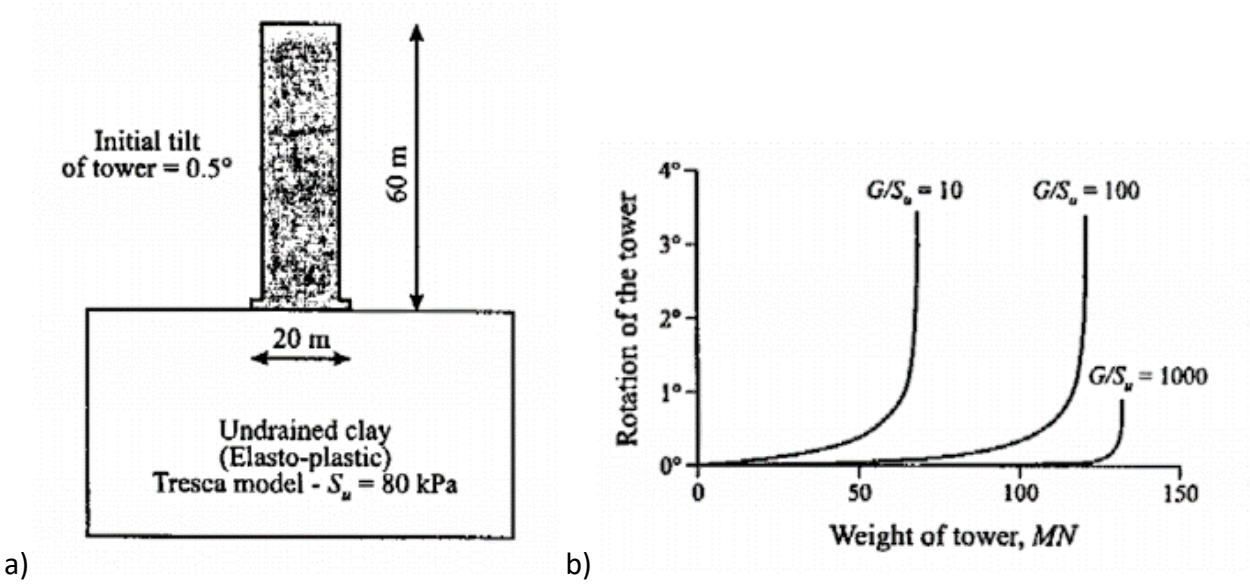

a) b)

Figure 2.11 Potts and Burland FEA (a) simulation of the plain strain problem

(b) inclination α of the tower versus weight for different soil stiffnesses

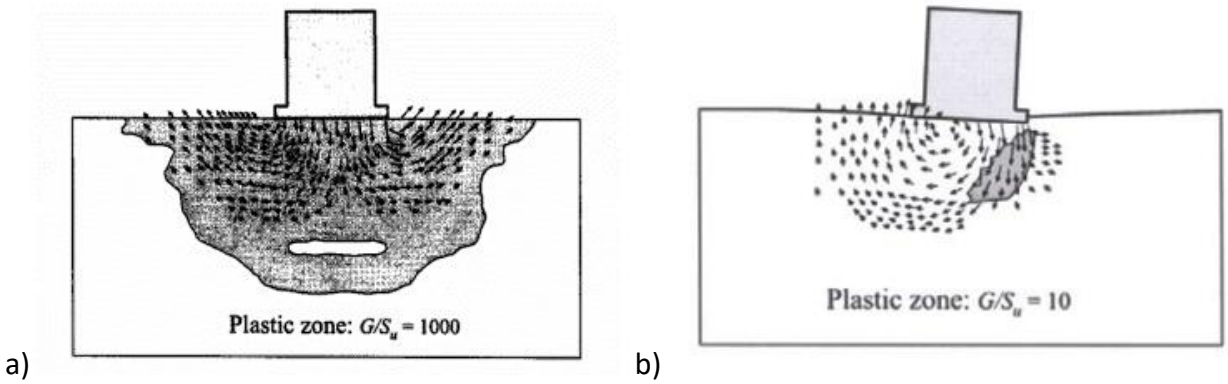

a) b)

Figure 2.12 Vectors of incremental displacement and extension of plastic zone at failure (a) in stiff clay, (b) in soft clay

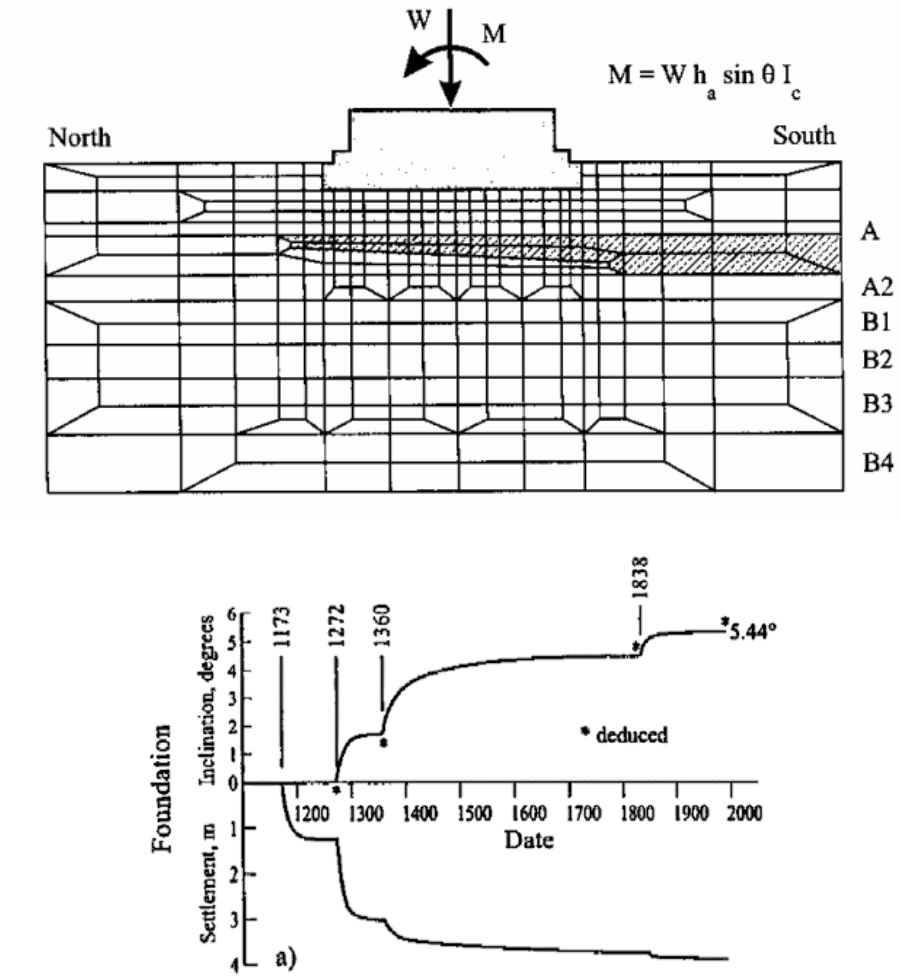

Figure 2.13 Finite element model (a) mesh in the vicinity of the tower foundation (b) comparison between the history of the tower and the results of the model

CHAPTER 3
STATIC ANALYSIS

3.1. STATEMENT OF THE PROBLEM

In this chapter we attempt to investigate the problem of the Tower of Pisa. In particular, we try to reach the current state of the Tower, defying simultaneously the mechanical behavior of its subsoil and the causes of its inclination. To this end, we performed a series of three dimensional static finite element analyses, using the Mohr-Coulomb constitutive model.

3.2. SIMULATION

We have carried out a 3D Finite Element Analysis of the behavior of the foundation of the Tower and its subsoil using the Abaqus code. Since the Tower does not tilt in the East-West direction, it is symmetric in the East-West plane. In order to reduce the number of elements of our model and consequently the time of analysis to half, we have cut our model in the middle in the plane of symmetry.

The footing is simulated as a rigid hollow cylinder with outer diameter equal to 20 m and inner diameter equal to 4 m. It is 3 m thick, equal to the overall depth of the foundation of the Tower. A rough approximation of the rate $\frac{D}{B} = \frac{3}{16} = 0.1875 < 0.5$ in addition with the fact that the footing is only partly embedded, due to the excavation of the catino, allows the representation of the footing as a shallow foundation. Considering, though, the positive effect of the surrounding ground, we assume a quite large Young's modulus equal to E=3000 GPa and a Poisson's ratio equal to v=0.15 to capture the rigid body motion of the footing. Due to the half model, the loads acting are the own weight of the footing (its density has been evaluated equal to ρ=1.73 Mgr/m^3) and half the weight of the superstructure, applied symmetrically with respect to the center of the

footing, in the form of two equal downward concentrated forces F=35.5 MN. The footing and its dimensions are depicted in figure 3.1.

The problem studied herein is axially symmetric, so the soil has been simulated as a cylinder in the center of which there is the footing. The depth of this cylinder is 40 m, since after this depth is laid the dense lower sand which does not contribute to the settlement of the Tower thanks to its strength. Additionally, as far as a circular foundation is concerned, the “stress bulb” starts to be negligible after a depth of 4 radii when a vertical load is acting and after a depth of 1.5 radii when an overturning moment is applied. Since the radius of the footing is equal to r=10 m, we can conclude that cylinder 40 m thick is sufficient and does not affect the results. The radius of the cylinder is equal to R=75 m. The subsoil in reality consists of 15 distinct layers, but in this simulation it is subdivided into 10 layers. In this way, we can reduce the complexity of the model and the time needed for the analysis, without affecting though the quality of the results, since the main ground profile and the layers that primarily contribute to the motions of the Tower have been taken into account thoroughly.

Both the footing and the soil are modeled with continuum solid plane strain 8-noded bilinear elements (C3D8). The mesh has been refined underneath the footing, in the immediate vicinity of the building, in order to obtain more reliable and detailed results in this area of interest. To be more specific, the elements in the whole of the cylinder have sides equal to 3 m except for those which constitute the refined mesh and have sides equal to 1m. The footing has the exact same mesh as the refined one that was described above. We have assumed a significantly large coefficient of friction, μ=1.8, at the soil-footing interface, in order to prevent sliding of the footing. Moreover, the lateral and bottom boundaries are fixed and the nodes on the plane of symmetry are not able to move out of range. The meshed model and its dimension are presented in figure 3.2.

3.3. SUBSOIL PROFILE

As mentioned above, the subsoil in our simulation is subdivided into 10 distinct layers, as shown in figure 3.3. Layer 1 and layer 2 are 2.5m and 3m thick respectively and they represent stratum

A1. Layer 3 refers to the medium dense sand layer of Horizon A and is 2m think. Layer 4 expands from 7.5m to 13m and represents deposits B1 and B2 of the Pancone clay, whereas stratum B3 is simulated by layer 5 and layer 6, which are 4m and 1m thick respectively. The stiffer "intermediate" clay and the "intermediate" sand, that means layers B4, B5 and B6 of Horizon B, are represented by the 6m thick layer 7. Strata B7, B8 and B9 that correspond to the first layers of the "lower" clay are simulated by layer 8, which is found to a depth from 24m to 34m, while the bottom layer B10 of the "lower" clay is represented by 4m thick layer 9. Finally, the first 2m of the "lower" dense sand are simulated by layer 10. It is to be noted that Horizon A and Pancone clay are simulated in a more detailed way, since they are mainly affected by the stress bulb and contribute to the movements of the Tower, while layers in bigger depths characterized by similar properties have been grouped together.

In order to realistically simulate the current state of the Pisa Tower, it is mandatory to correct the soil properties as defined by the geotechnical investigations described in chapter 2, and particularly the small strain shear modulus G_{max} and the undrained shear strength S_u. To be more specific, only a few tests have been carried out beneath the Tower of Pisa to assess the soil characteristics, while most of the results refer to boreholes conducted beyond its periphery. As a result, the consolidation of the soil under the weight of the Tower has not been taken into account, leading to reduced values of G_{max} and S_u. Considering that the expression $G_{vh}=480\cdot e^{-1.43}\cdot \sigma_v^{'0.22}\cdot \sigma_h^{'0.22}\cdot p_a^{0.56}$ can be used for all the subsoil layers and assuming that changes in void ratio due to consolidation are not significant, we used the next equations to achieve our goal:

$$G_{max,n}=G_{max,o}\cdot\left(\frac{\sigma_{v,f}}{\sigma_{v,0}}\right)^{0,22}\cdot\left(\frac{\sigma_{h,f}}{\sigma_{h,0}}\right)^{0,22}$$

$$S_{u,n}=S_{u,o}\cdot\left(\frac{\sigma_{v,f}}{\sigma_{v,0}}\right)^{0,22}\cdot\left(\frac{\sigma_{h,f}}{\sigma_{h,0}}\right)^{0,22}$$

where $\sigma_{v,f}$, $\sigma_{h,f}$ are the total vertical and horizontal stresses after the construction of the Tower, and $\sigma_{v,0}$, $\sigma_{h,0}$ are the total vertical and horizontal geostatic stresses. The stresses have been obtained by carrying out Finite Element Analysis with Abaqus, considering at first only the stresses developed due to the own weight of the subsoil and then those developed after applying the

weight of the foundation and the superstructure. In this analysis, the soil properties are those defined in chapter 2, while mean values were used where needed, such as in the case of grouped layers. The small strain shear modulus of the soil was calculated from the shear wave velocity and the density of the soil using the expression $G_{max,0}=\rho \cdot V_s^2$, where the saturated density of the soil is that shown in the following table:

DEPTH z (m)	DENSITY ρ (Mgr/m^3)
0-7.5	1.85
7.5-18	1.7
18-24	1.9
24-34	1.87
34-38	1.9
38-40	2

and the profile of Vs is shown in figure 3.4.The corrected profiles of the maximum shear modulus and the undrained shear strength together with the initially used values are plotted in figures 3.5(a) and 3.5(b) respectively.

3.4. ELASTIC ANALYSIS

Attempting to monitor our model behavior and confirm its validity, we have carried out Finite Element Analyses, assuming the subsoil to be an elastic material. In these analyses the only properties needed to define the behavior of the soil are the Young's modulus E and the Poisson's ratio v. Since we assume undrained conditions in our simulation, we choose a Poisson's ratio v=0.48, while the Young's modulus is calculated using the expression $E=2 \cdot G \cdot (1+v)$. Considering that the maximum shear modulus corresponds to stiff soil with small shear strain, whereas the subsoil is subjected to quite large deformations that exceed the area of elastic response, we conclude that the maximum value of shear modulus G_{max} is not appropriate to represent the stiffness of the soil. As a result, we carried out analyses considering reduced values of the shear modulus as a parameter. To be more specific, we have tested the profiles $G_{max}/5$, $G_{max}/50$ and $G_{max}/100$ that refer to a stiff, intermediate and very soft soil respectively.

It is obvious that in elastic analyses, since the subsoil does not yield, failure will occur only when the overturning moment, generated due to the eccentricity of the center of gravity of the Tower, becomes slightly bigger than the resisting moment generated by the rotational stiffness of the ground. For each soil profile of those mentioned above we applied on the footing an overturning moment in the form of two equal concentrated forces F of a distance d (one downward and one upward), applied symmetrically with respect to the center of the footing ($M_r = F \cdot d$). We carried out analyses increasing each time the value of the forces F, until the applied moment M_r reached the overturning moment due to the Tower weight M_o, and calculating the resulting rotation θ of the footing, so as to obtain the rotation-moment curve of the subsoil. For the analyses where $M_r = M_o$ we determined the resulting stresses and deformations of the subsoil, so as to examine its response and evaluate its behavior.

The results obtained by the followed procedure are plotted in diagrams which are presented at the end of this chapter. To be more specific, the rotation angle of the Tower as the applied moment increases for each one of the tested soil profiles is depicted in figure 3.6. Vertical stresses with depth on the south edge, on the axis of symmetry and on the north edge of the footing are plotted in figures 3.7, 3.8 and 3.9 respectively. These diagrams can be divided into two subcategories:

1) Those which depict total stresses due to both the geostatic stresses and the stresses caused by the weight of the Tower and the moment applied due to its inclination. In this case, the lines of stress distribution for geostatic condition are also plotted, to provide a better conception of the evolution of stresses.

2) Those which depict only the additional stresses due to the weight of the Tower and the overturning moment, for the better comprehension of the affection of the applied loads.

Moreover, we plotted vertical stresses on the soil surface and on the surface of the Pancone clay, shown in figures 3.10 and 3.11 respectively. Again the diagrams are grouped as mentioned above. Finally, figure 3.12 presents the deformed shape of the soil surface as computed from Abaqus with contours and graphic representation, while the settlement of the soil surface and the settlement of the surface of Pancone clay are shown in figures 3.13 and 3.14 respectively.

The assessment of the results that came of our analyses leads to some important conclusions considering the validity of the model. First of all, as was expected, the elastic analysis cannot represent the current state of the Tower, since the desired rotation and settlement, meaning those that adequately approach the real values of the Tower's movements, are achieved for an extremely soft soil ($G_{max}/100$), that is not the case for Pisa subsoil. In general, the softer the soil is, the bigger final rotation angle of the footing and settlement of the ground are observed, as expected. Moreover, a closer look at the diagram of settlement of Pancone clay surface, compared to that of the soil surface, indicates that the "upper" clay has quite large settlements that significantly contribute to the movements of the Tower. As far as the vertical normal stresses are concerned, they are approximately equal for each of the different soil profiles, confirming the fact that shear modulus G affects minimally the normal stresses, while the shear stresses are affected dramatically. Finally, it should be mentioned that the distribution of vertical normal stresses on the surface of the soil aggrees on some point with the distribution predicted theoritically by elasticity theory, since stresses at the corners of the footing are signifficantly bigger than those under the footing. On the hole, the behavior of our model seems to be of high quality and the results expected to be reliable.

3.5. MOHR-COULOMB

The Mohr-Coulomb failure or strength criterion has been widely used for geotechnical applications. It is based on Coulomb's observation that all the materials derive strength from two sources, cohesion and friction, and that failure will usually be associated with a surface of rupture within the soil mass. According to this criterion, yield occurs when the shear stress on any point in a material reaches a maximum value that depends linearly on the normal stress in the same plane:

$$\tau = c + \sigma \tan\phi$$

where τ and σ represent the shearing stress and normal stress on the physical plane through material failure occurs. The constant c is the cohesion and the angle ϕ is the angle of internal friction of the soil.

If failure is to occur for a combination of principal stresses $\sigma_1 \geq \sigma_2 \geq \sigma_3$, the critical Mohr stress circle, derived from σ_1 and σ_3 must be a tangent to the line generated by the yield criterion as

shown in figure 3.15. Consequently, we can relate the values of τ and σ to the principal stresses as follows:

$$\tau = \frac{1}{2} \cdot (\sigma_1 - \sigma_3) \cdot \cos\varphi$$

$$\sigma = \frac{1}{2} \cdot (\sigma_1 + \sigma_3) - \frac{1}{2} \cdot (\sigma_1 - \sigma_3) \cdot \sin\varphi \ .$$

Then we can rewrite the Mohr-Coulomb criterion in terms of principal stresses:

$$\sigma_1 \cdot (1-\sin\varphi) - \sigma_3 \cdot (1+\sin\varphi) = 2 \cdot c \cdot \cos\varphi$$

Obviously, yielding does not depend upon the intermediate principal stress σ_2. If we plot the Mohr-Coulomb yield surface in the π-plane, we deduce that Coulomb's criterion depends on the mean stress p. Therefore the surface has an expanding pyramid shape with a cross-section that is an irregular hexagon as shown in figure 3.16.

In order to simulate the current state of the Tower, we assumed Mohr-Coulomb plastic behavior for the subsoil layers and carried out finite element analyses considering undrained conditions. As mentioned in the previous paragraph, the subsoil is subjected to quite large deformations that exceed the area of elastic response, which means that the maximum value of shear modulus G_{max} is not appropriate to represent the stiffness of the soil. As a result, again we carried out analyses considering reduced values of the shear modulus G and undrained shear strength S_u as parameters. The values of G-S_u pair of profiles that were tested are the following: the determined by the Polvani and International Committees profiles (G, S_u), the reduced profiles (90%G, 80% S_u) and the reduced profiles (95%G, 90% S_u).

The criteria for the choice of the properties that represent the soil behavior are the resulting settlement of the ground, the rotation of the footing and the resisting moment of the subsoil that fit in the best way the real values of the referring parameters. We should notice that the moment due to the rotational stiffness of the subsoil should be equal to the overturning moment due to the weight of the Tower, since, as it is known, the safety factor is very close to 1. In order to examine the above, we apply an overturning moment on the footing in the same way as in the elastic analysis. We carried out analyses for many different values of the forces F and calculated the resulting rotation θ of the footing, so as to obtain the rotation-moment curve of the subsoil.

This curve was plotted in the same diagram with the overturning moment $M_0 = W \cdot h_c \cdot \theta$ generated by the weight of the Tower as a function of its angle of rotation θ, in order to determine the intersection point of the two curves. The diagrams that came of the prescribed procedure for each pair of (G, S_u) profiles are plotted in figure 3.17. Since our goal is to approach the real overturning moment M=327 MNm and the rotation angle of the Tower θ=5.5˚, it is obvious that a shear modulus equal to 95%G and an undrained shear strength equal to 90%S_u, that result in a resisting moment M_r=344MNm and an angle of rotation θ=6.17˚, sufficiently represent the current soil properties.

Subsequently, in order to obtain an overview of the model behavior and evaluate the quality of the selected properties, we present the resulting stresses and deformations of the subsoil in the form of diagrams for several areas of interest. To be more specific, vertical stresses with depth on the south edge, on the axis of symmetry and on the north edge of the footing are plotted in figures 3.18, 3.19 and 3.20 respectively. Moreover, we plotted vertical stresses on the soil surface in figure 3.21 and on the surface of the Pancone clay in figure 3.22. Figures 3.23-3.25 illustrate horizontal stresses with depth on the south edge, on the axis of symmetry and on the north edge of the footing. As in the elastic analysis, the diagrams present both total and additional stresses. In figure 3.26 is depicted the deformed shape of the soil surface under the weight of the Tower, while figure 3.27 presents the zone under the footing that has been plasticized, as obtained from Abaqus with contours. Finally, the settlement of the soil surface and the surface of Pancone clay are shown in figures 3.28 and 3.29 respectively.

As far as the resulting diagrams are concerned, some important observations should be pointed out. First of all, from the figure that illustrates the zone of fully mobilized strength, we deduce that failure does not occur and the Tower, which is really close to leaning instability, since the resistance moment M_r is almost equal to the overturning moment M_0, is subjected to a significant rotation without collapsing. Moreover, stress distribution under the footing indicates the concentration of stresses to its southern corner, where stresses due to the Tower weight and those due to the overturning moment have the same direction, while tensile stresses are observed at the north corner, since the footing has been lifted up. At the axis of symmetry stresses on the soil surface are zero, which is explained due to the existence of the hole of the footing and,

therefore the fact that no load is applied in that area. Generally, stresses southern of the axis of the footing are greater than those developed northwards resulting in bigger settlements of the subsoil. More specifically, as indicated by the deformed shape of both the soil surface and the "upper" clay surface, the soil under the Tower is subjected to differential settlements, since those at the south are bigger. Once again, we observe that the settlement of the Pancone clay, except for asymmetric, is quite large too, leading to the conclusion that it significantly affects both the tilting and the settlement of the Tower.

FIGURES OF CHAPTER 3

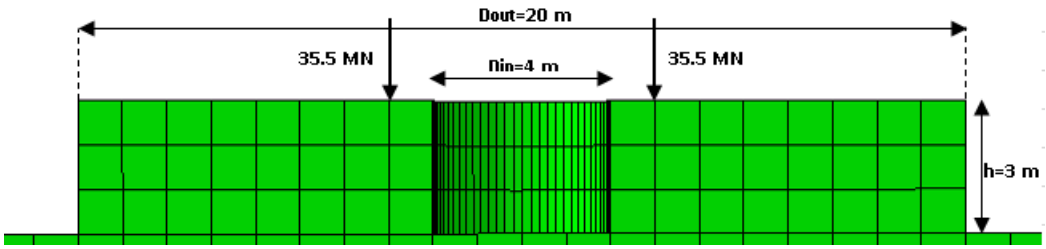

Figure 3.1 Dimensions of the footing

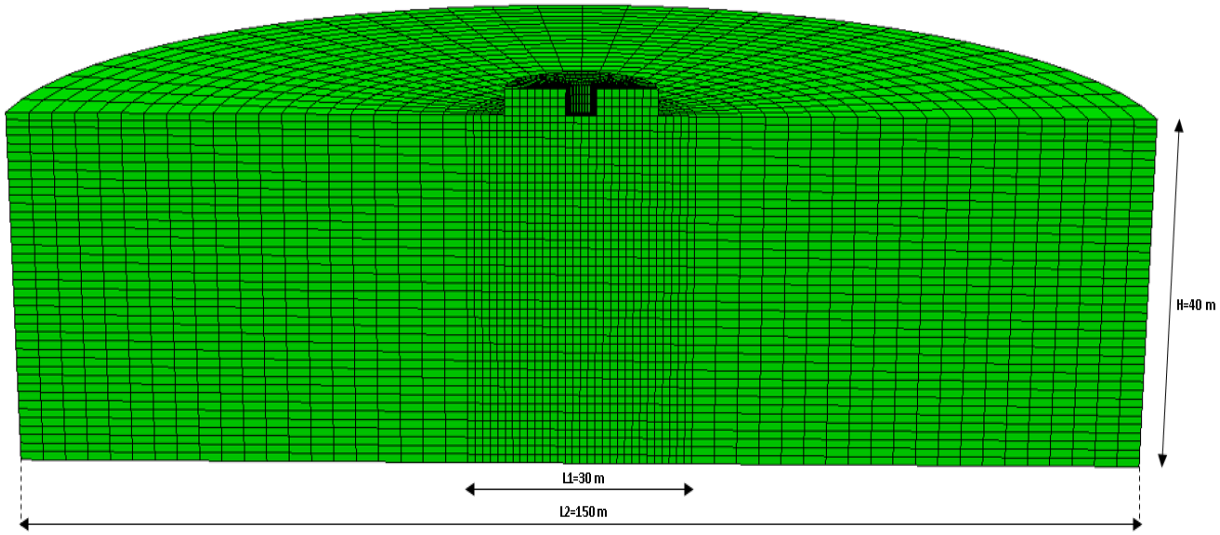

Figure 3.2 Dimensions and meshing of the model

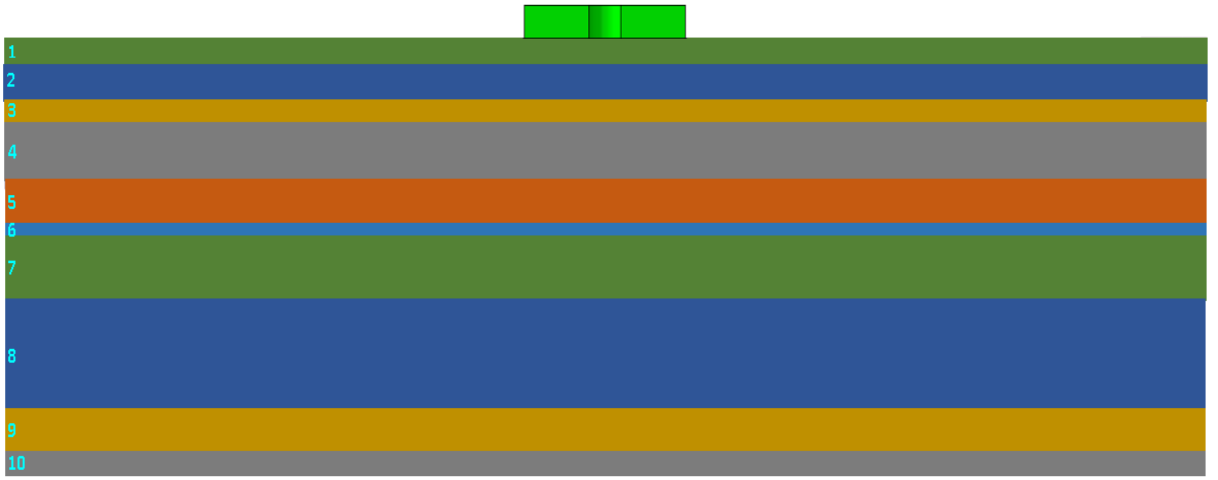

Figure 3.3 Layers of the subsoil

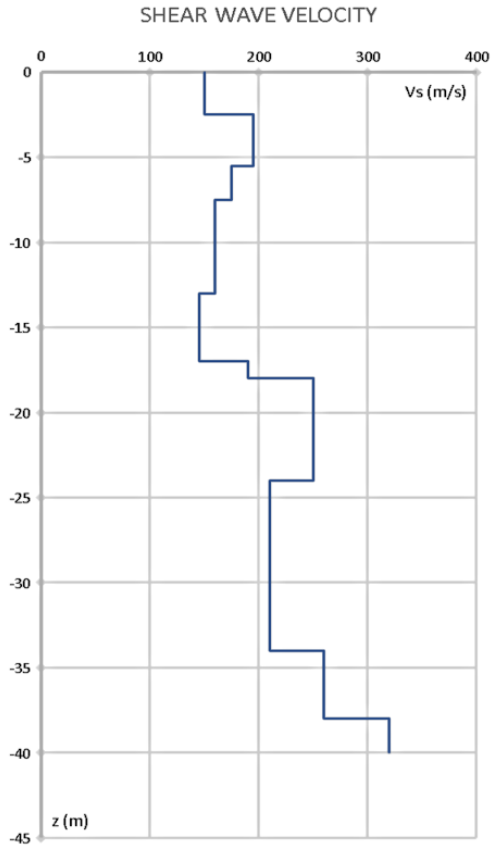

Figure 3.4 Shear wave velocity profile, as measured by means of in situ seismic methods

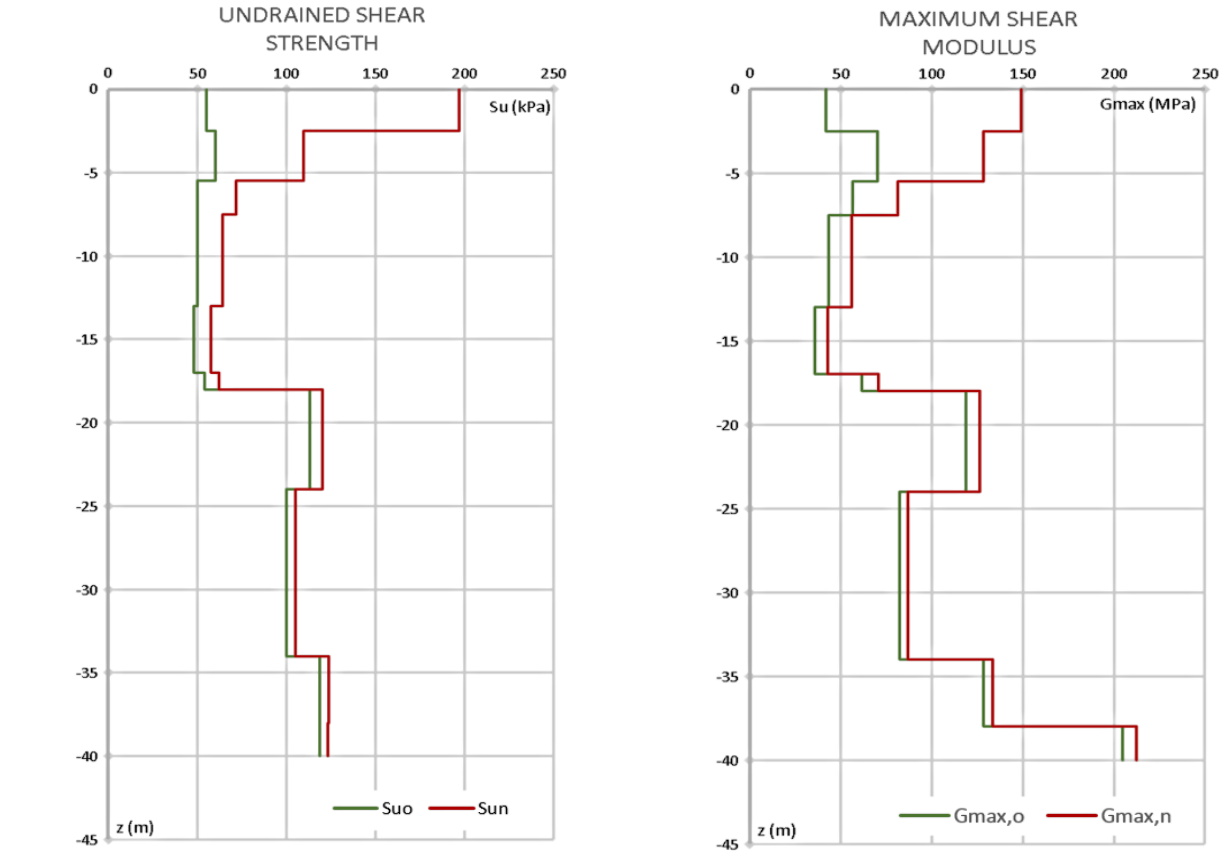

a) b)

Figure 3.5 Profiles of a) undrained shear strength, b) small strain shear modulus before and after correction due to soil consolidation under the Tower weight

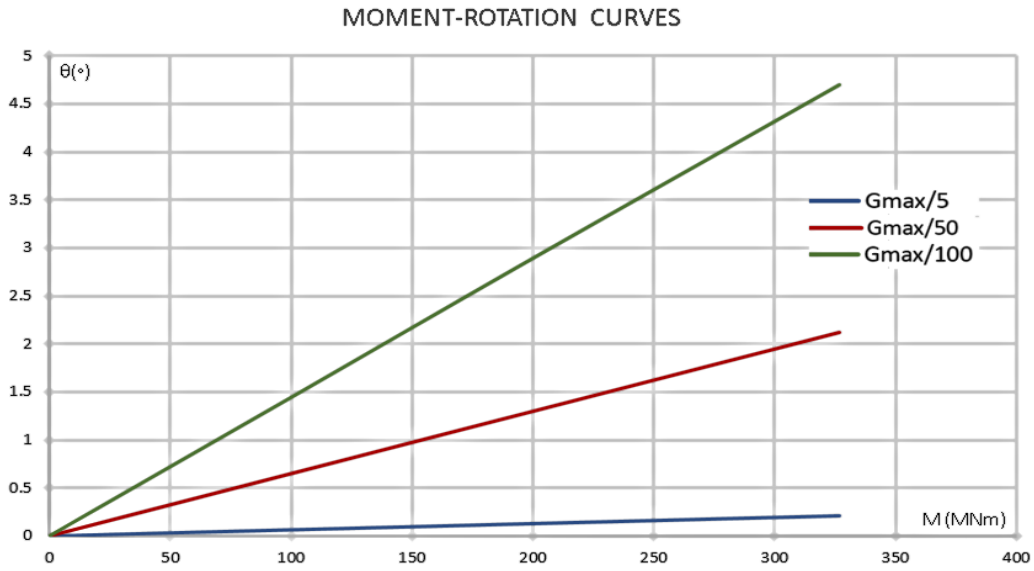

Figure 3.6 Moment-Rotation curves for various shear modulus G

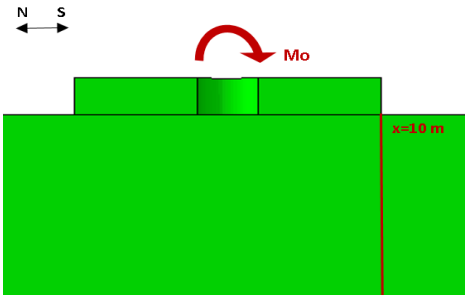

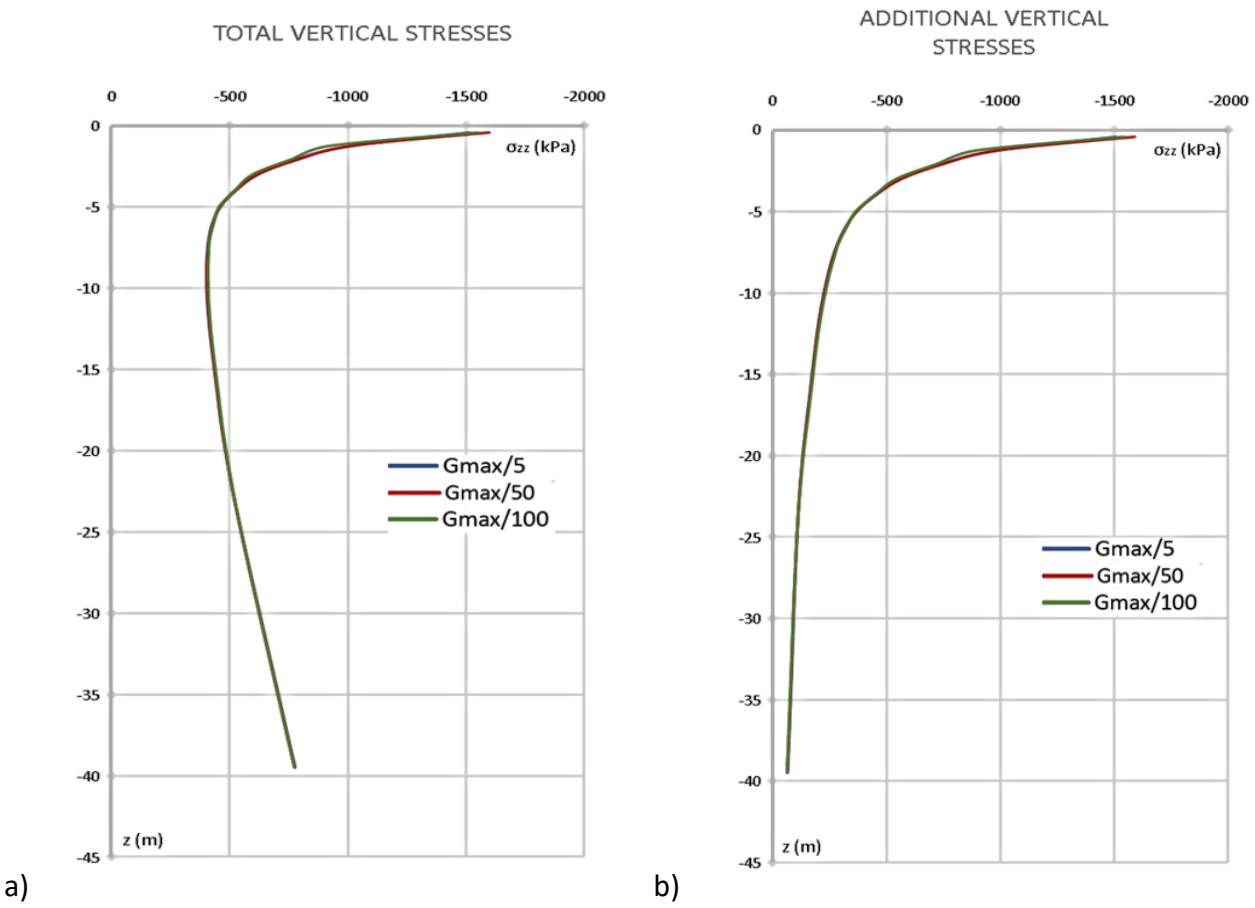

Figure 3.7 Distribution of a) total vertical and b) additional vertical stresses with depth for various shear modulus

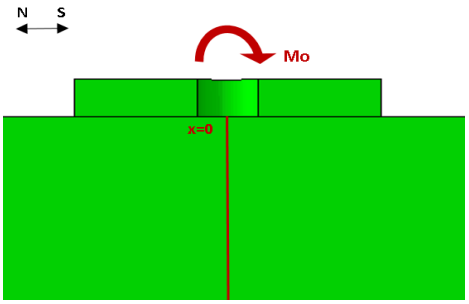

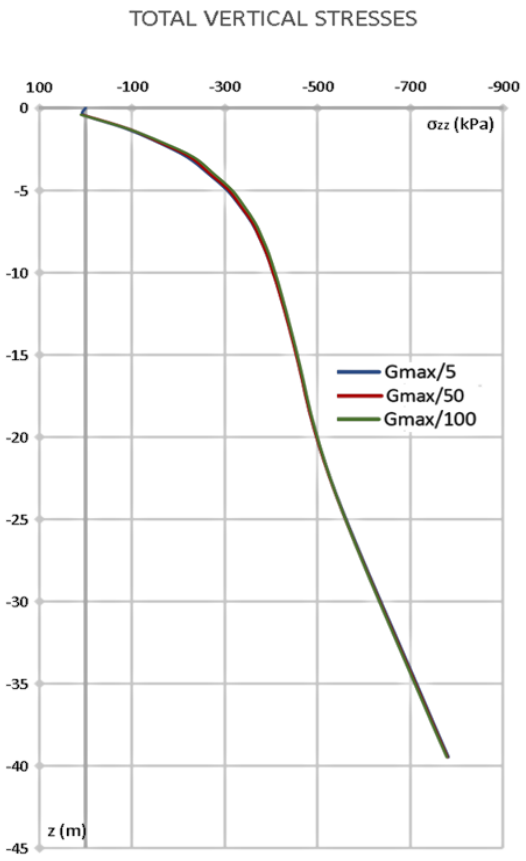

a)

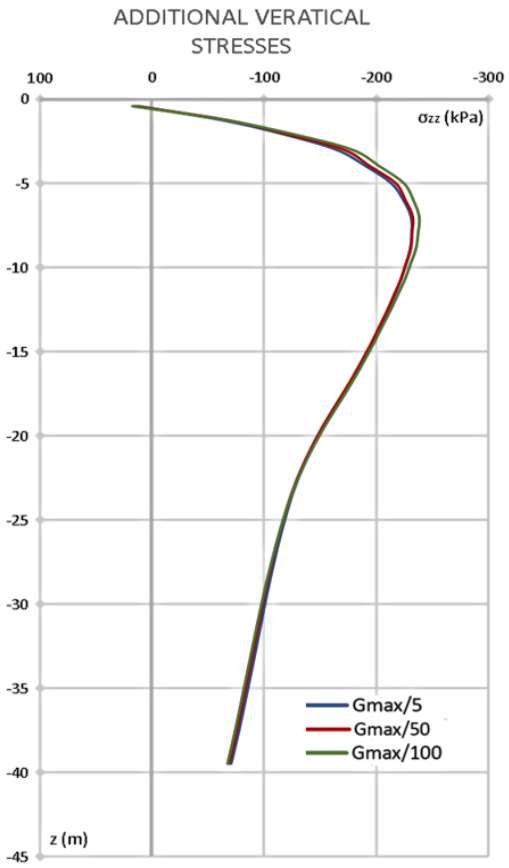

b)

Figure 3.8 Distribution of a) total vertical stresses and b) additional vertical stresses with depth for various shear modulus

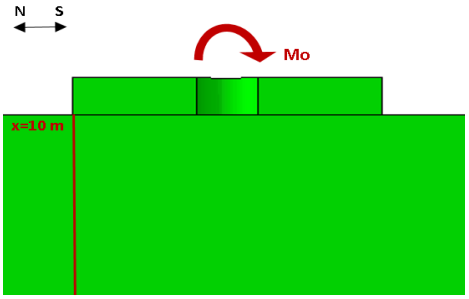

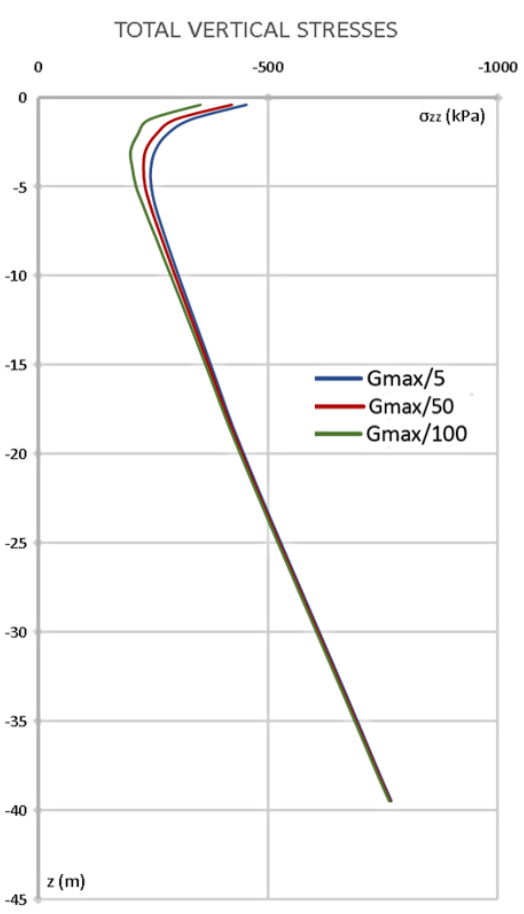

a)

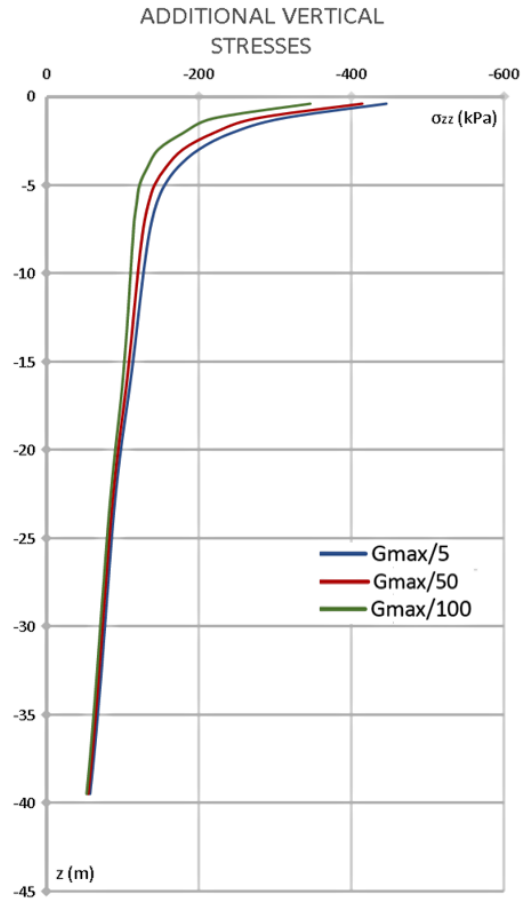

b)

Figure 3.9 Distribution of a) total vertical stresses and b) additional vertical stresses with depth for various shear modulus

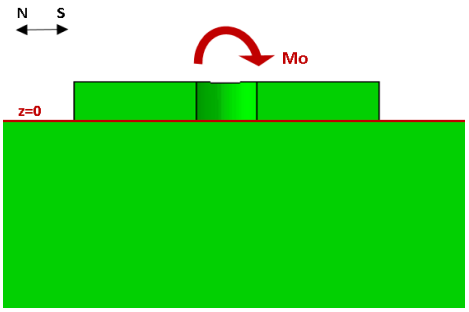

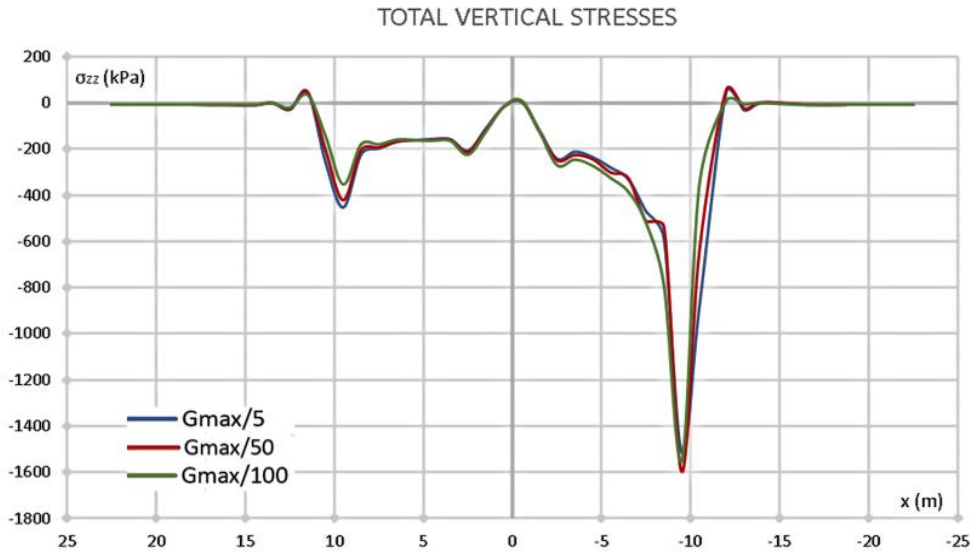

a)

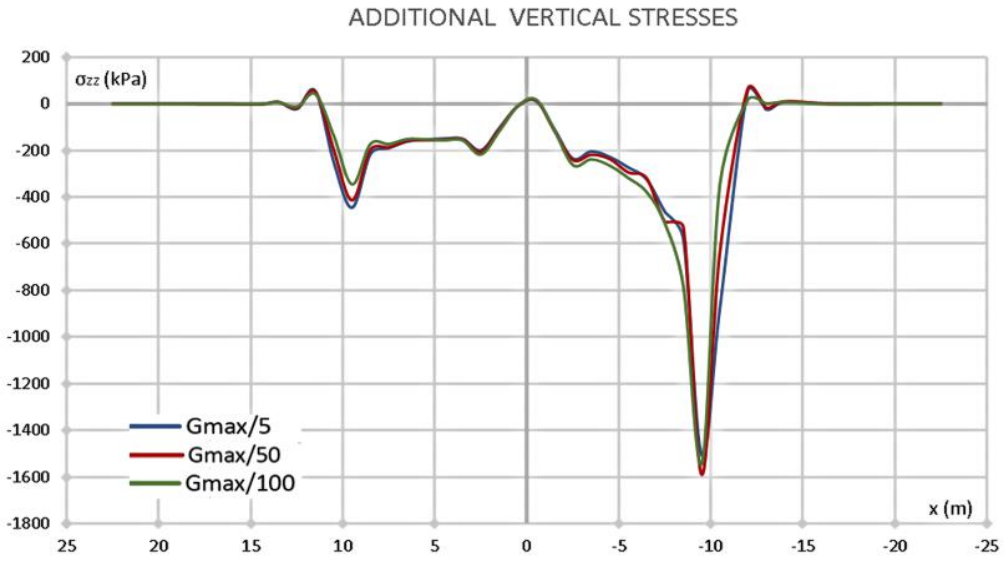

b)

Figure 3.10 Distribution of a) total vertical stresses and b) additional vertical stresses on soil surface for various shear modulus

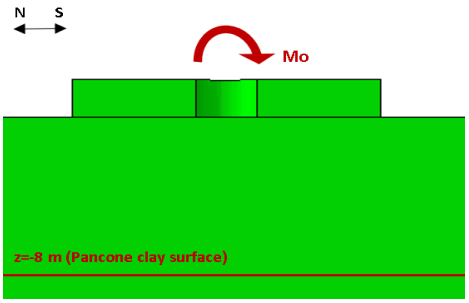

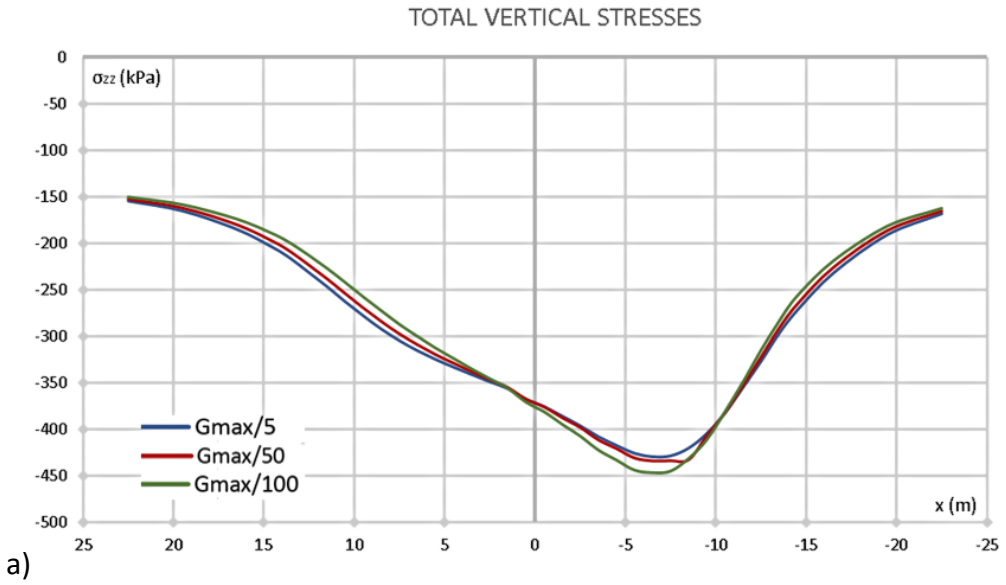

a)

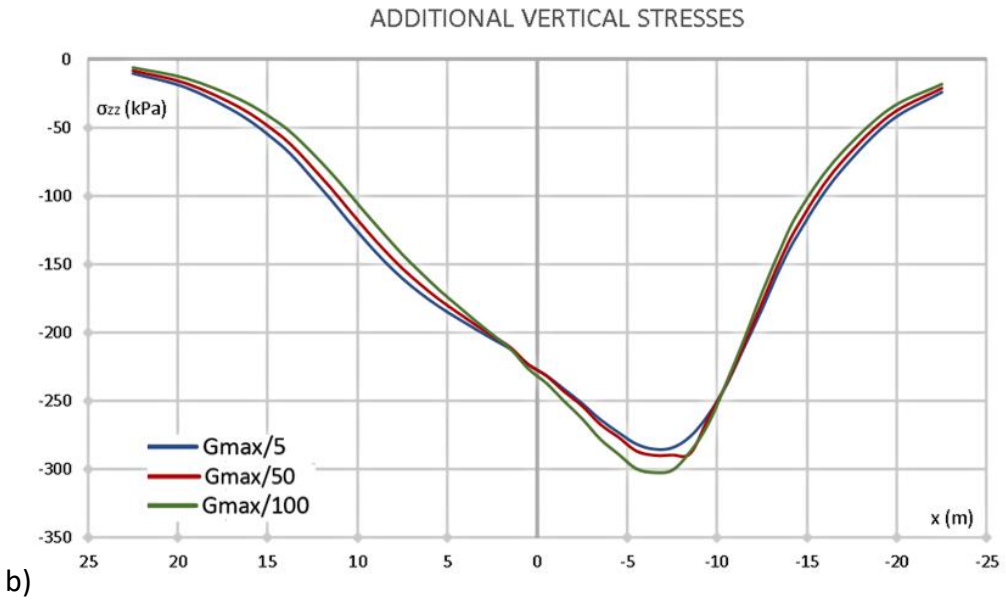

b)

Figure 3.11 Distribution of a) total vertical stresses and b) additional vertical stresses on Pancone clay surface for various shear modulus

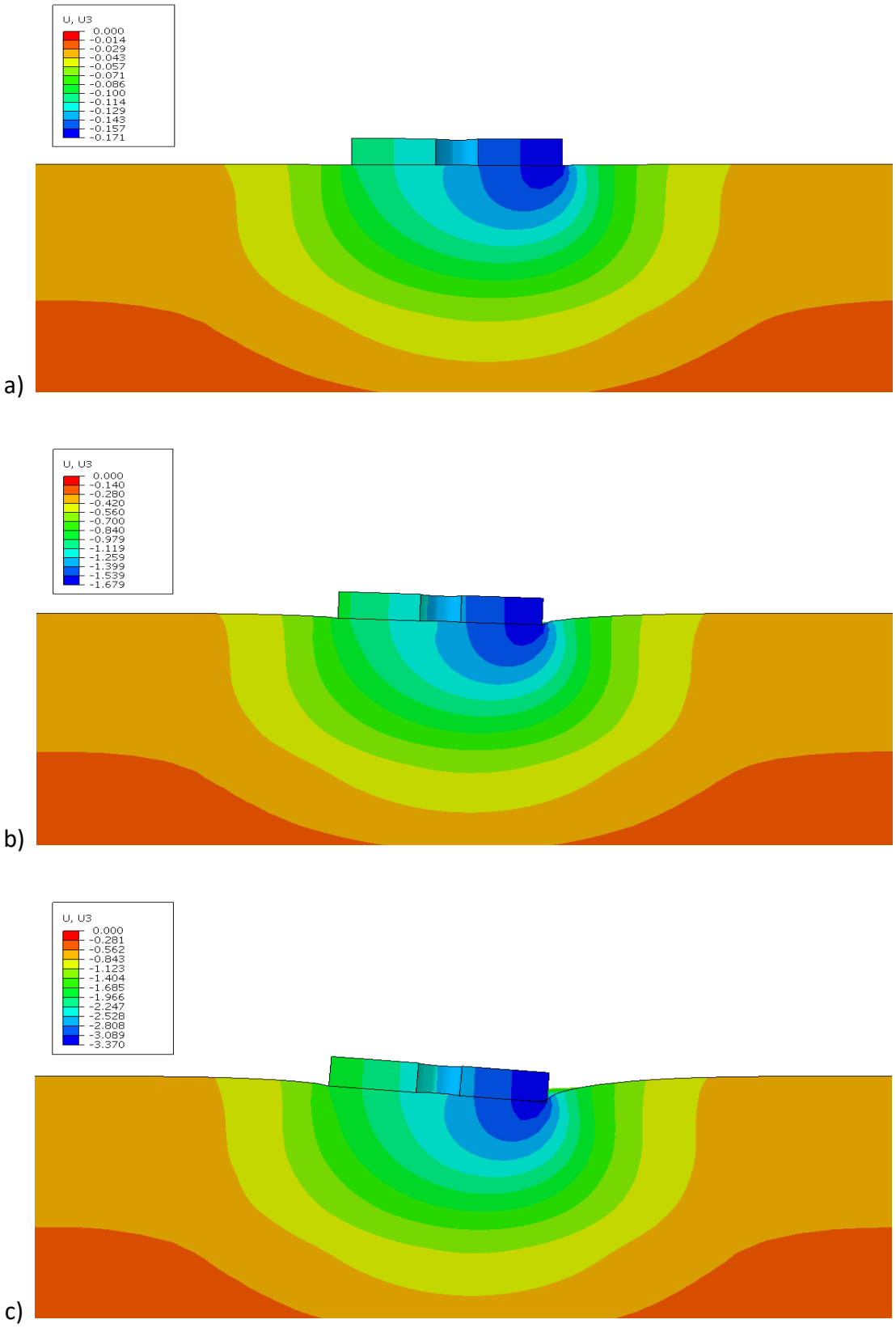

Figure 3.12 Deformed shape of the surface of the soil for shear modulus

a) $G_{max}/5$, b) $G_{max}/50$, c) $G_{max}/100$ as depicted from Abaqus with contours settlement

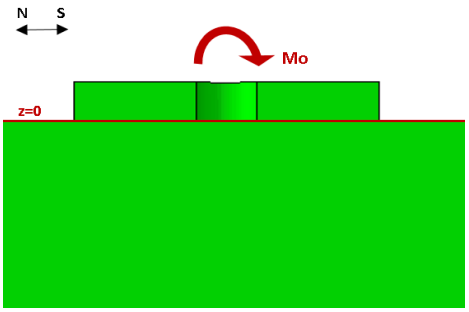

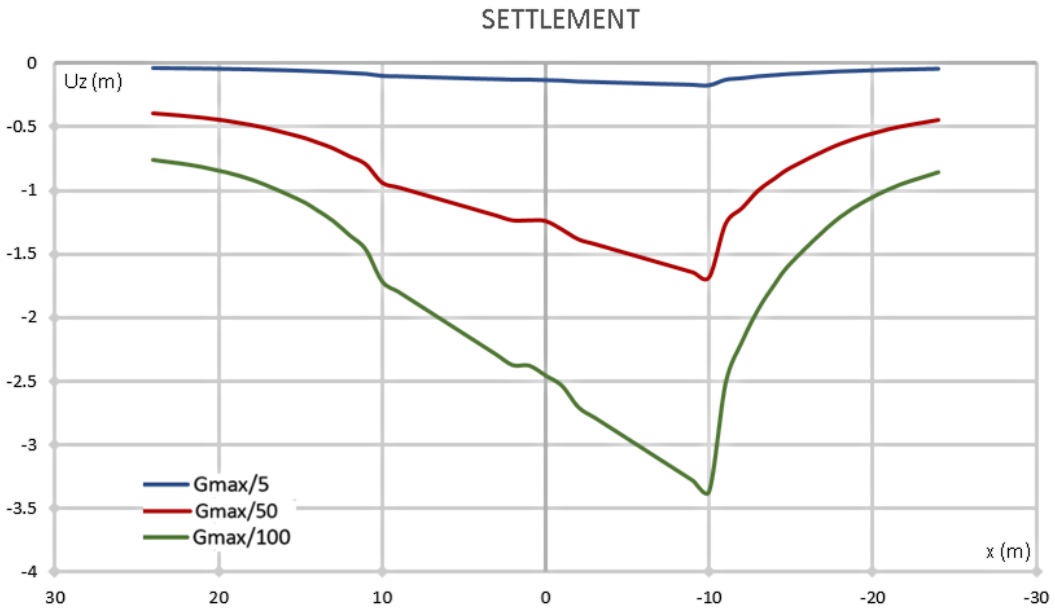

Figure 3.13 Settlement of the surface of the soil for various shear modulus

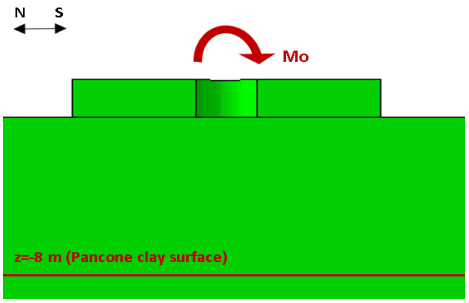

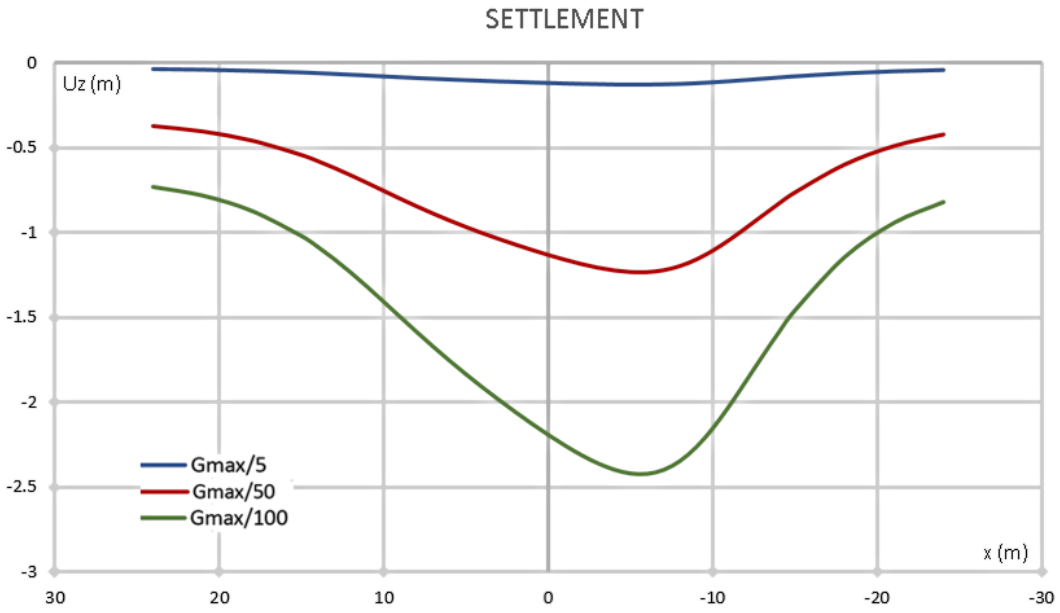

Figure 3.14 Settlement of the surface of Pancone clay for various shear modulus

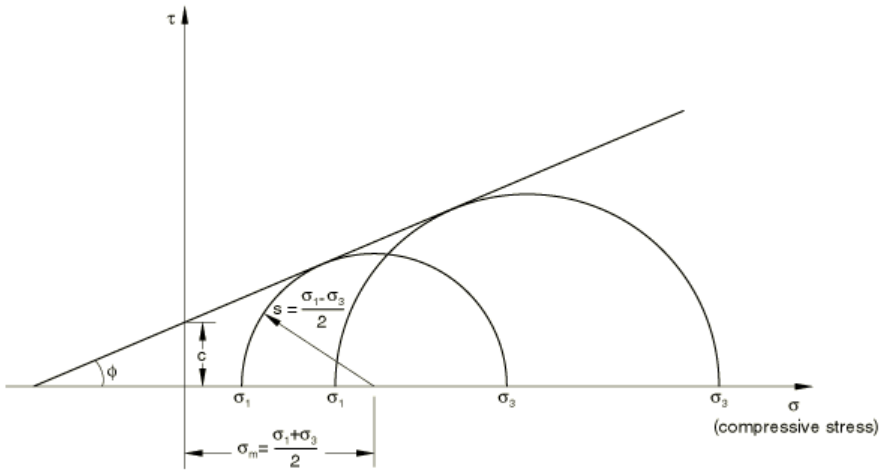

Figure 3.15 The Coulomb failure criterion

Figure 3.16 Perspective view of the Coulomb yield surface

a)

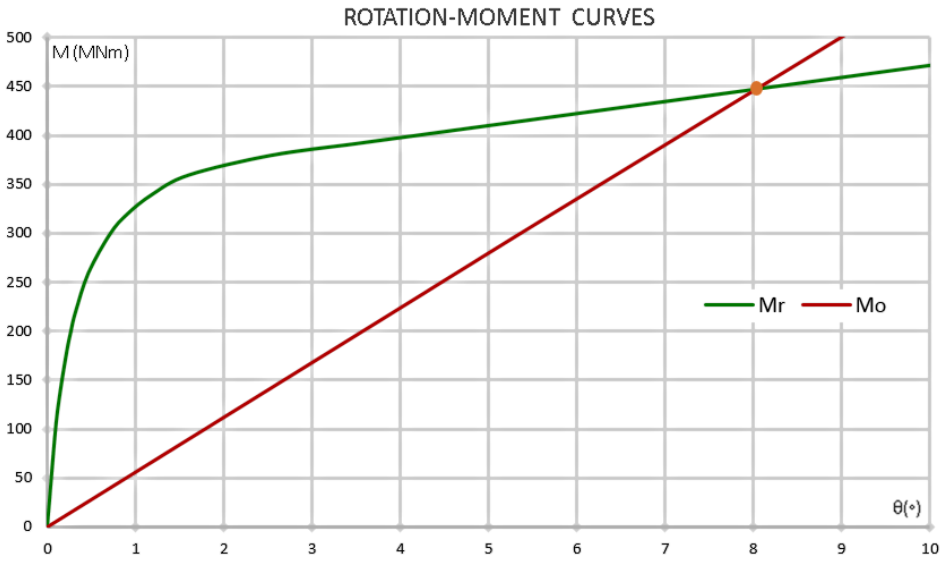

b)

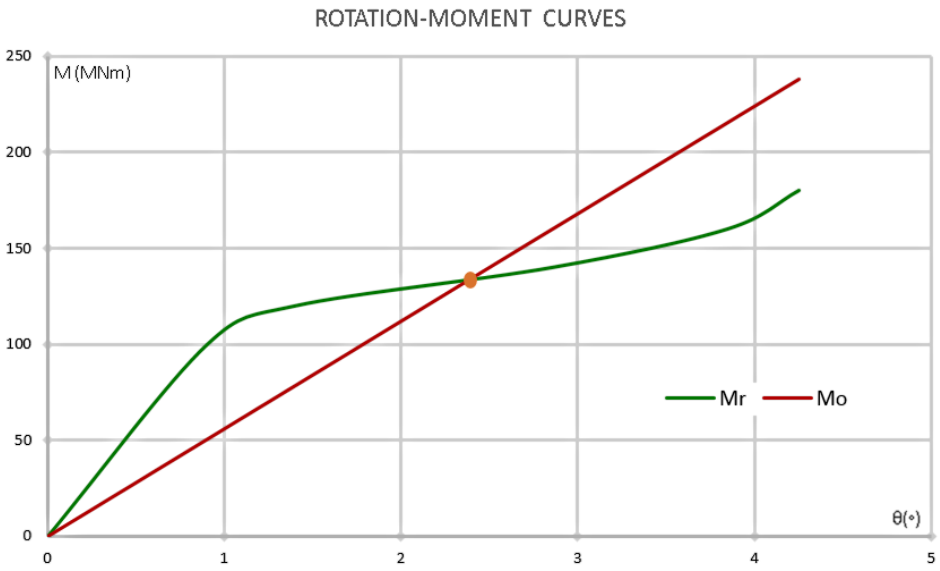

c)

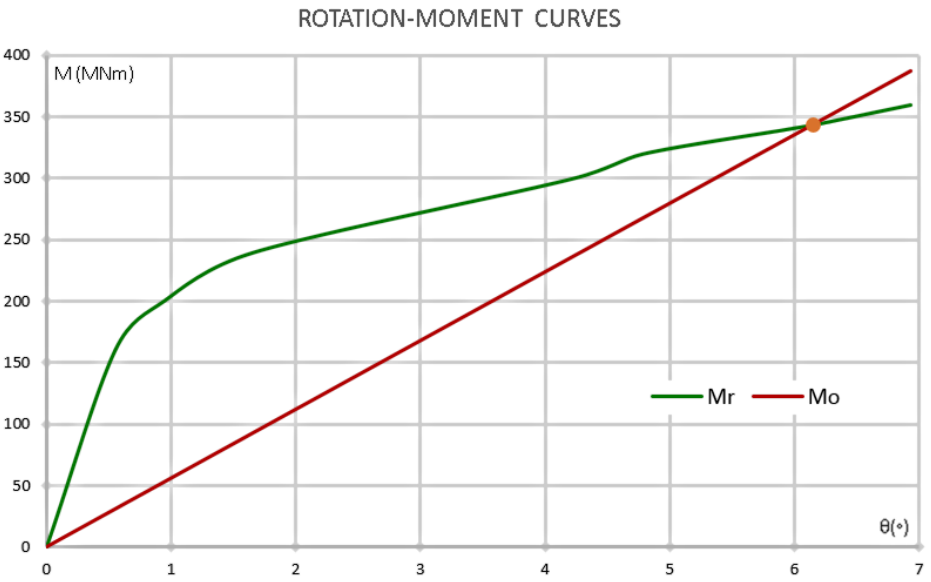

Figure 3.17 Rotation-Moment curves for various subsoil profiles:

a) G-S_u, b) 90%G-80%Su, c) 95%G-90%Su

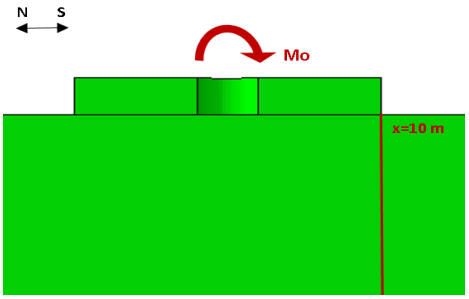

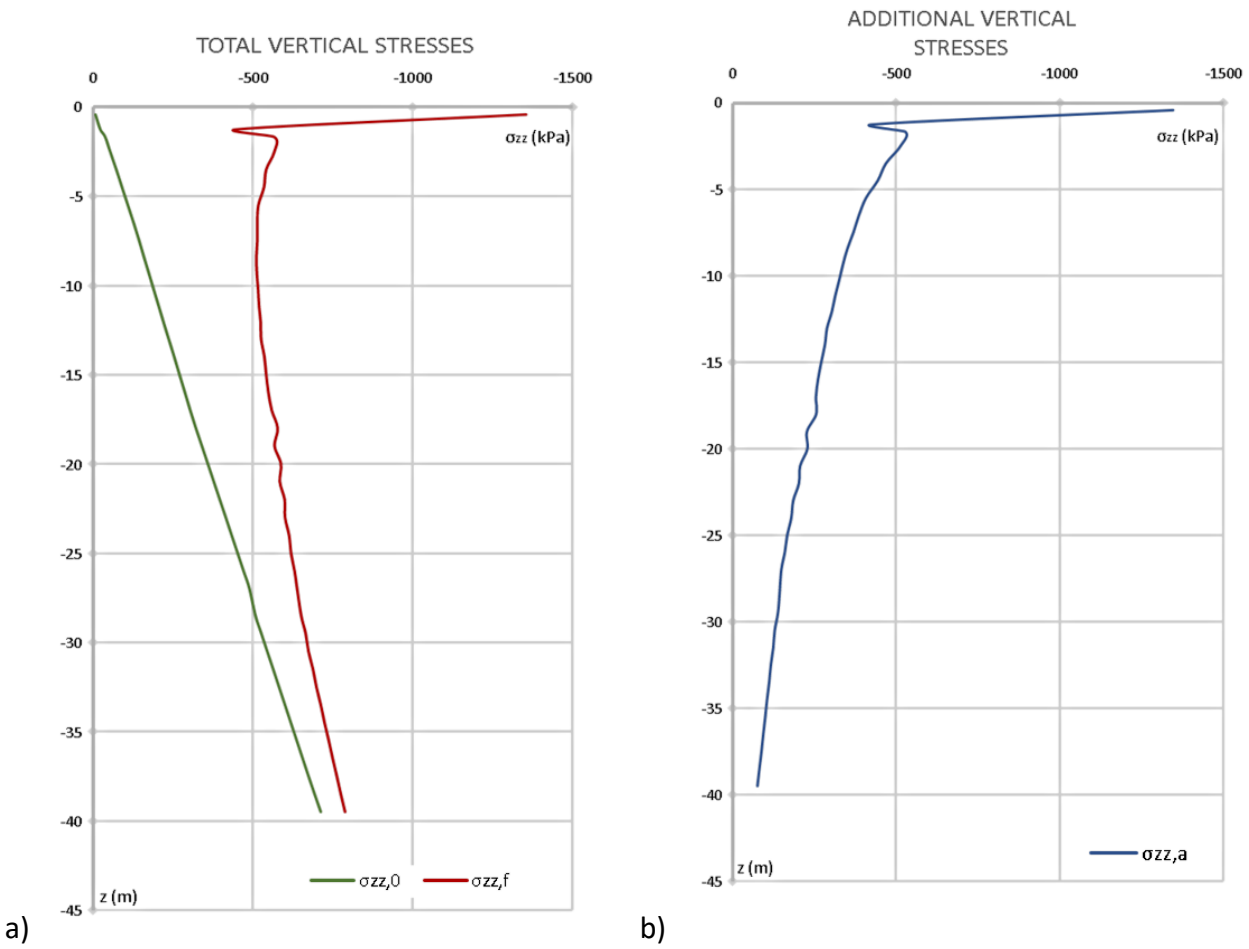

a) b)

Figure 3.18 Distribution of a) total vertical stresses and b) additional vertical stresses with depth for 95%G, 90%S_u

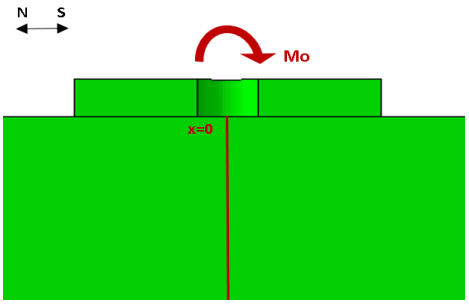

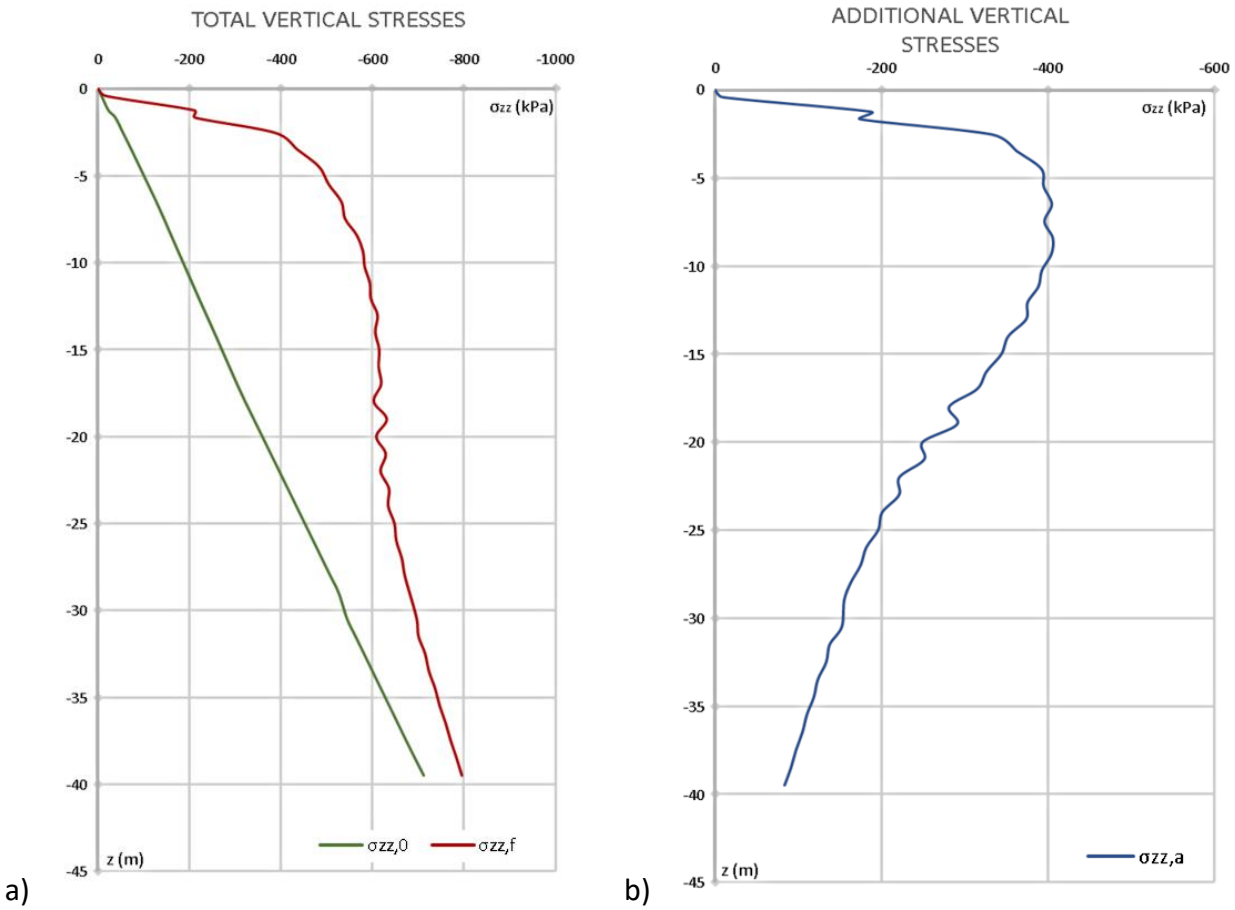

Figure 3.19 Distribution of a) total vertical stresses and b) additional vertical stresses with depth for 95%G, 90%S_u

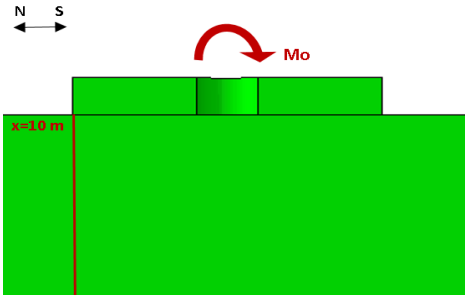

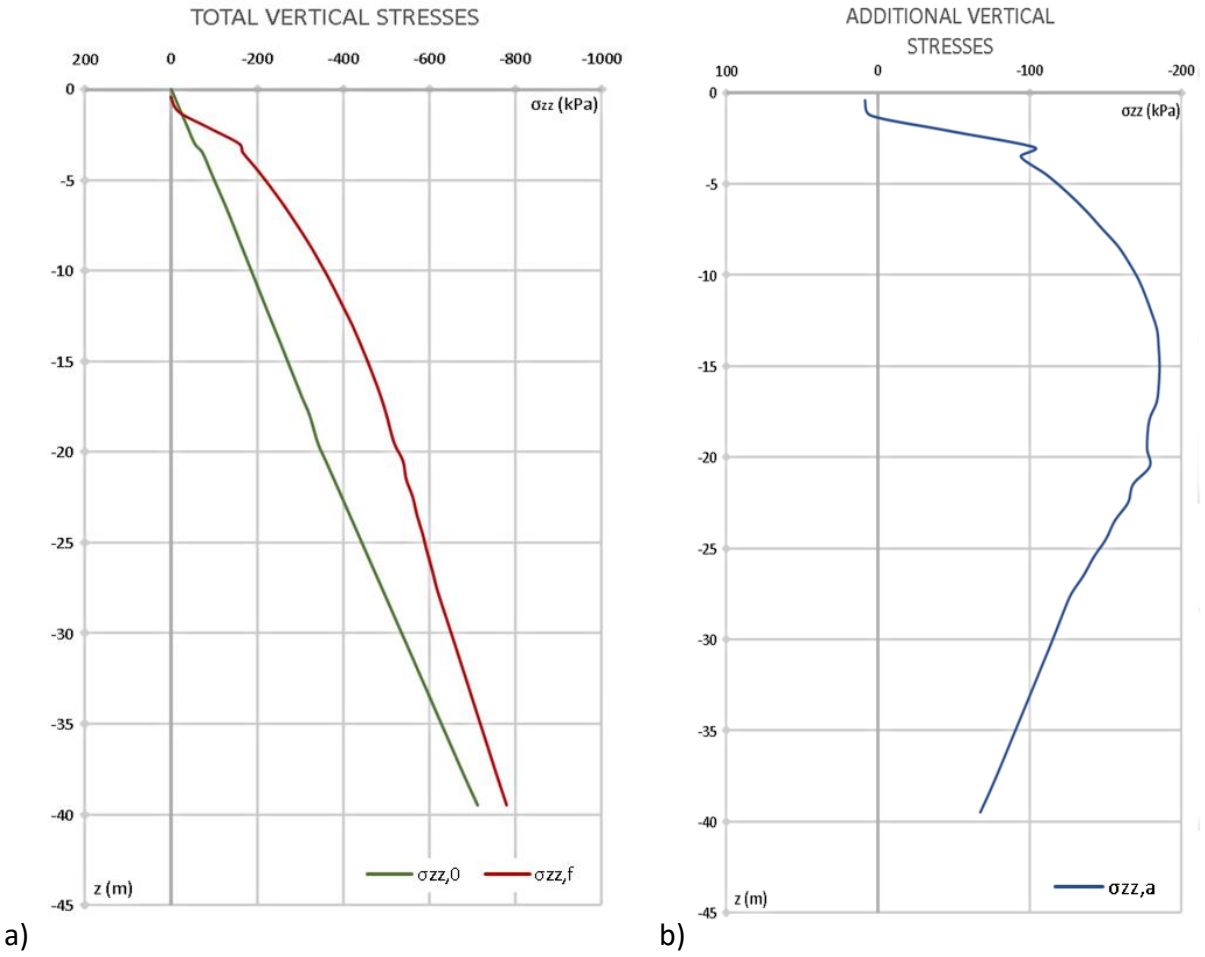

a) b)

Figure 3.20 Distribution of a) total vertical stresses and b) additional vertical stresses with depth for 95%G, 90%S_u

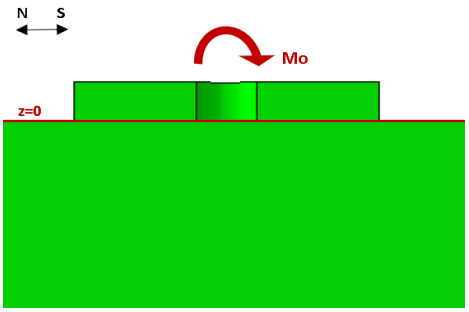

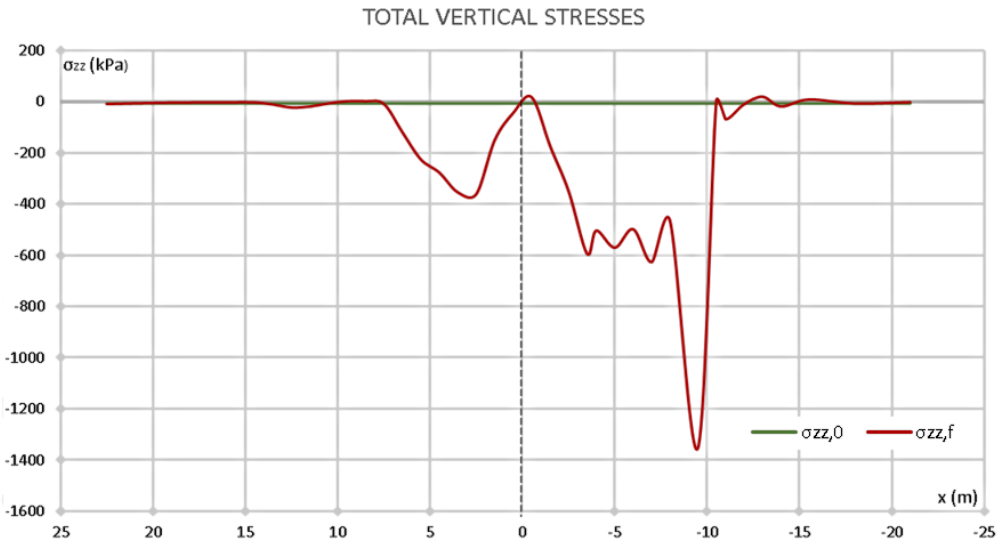

a)

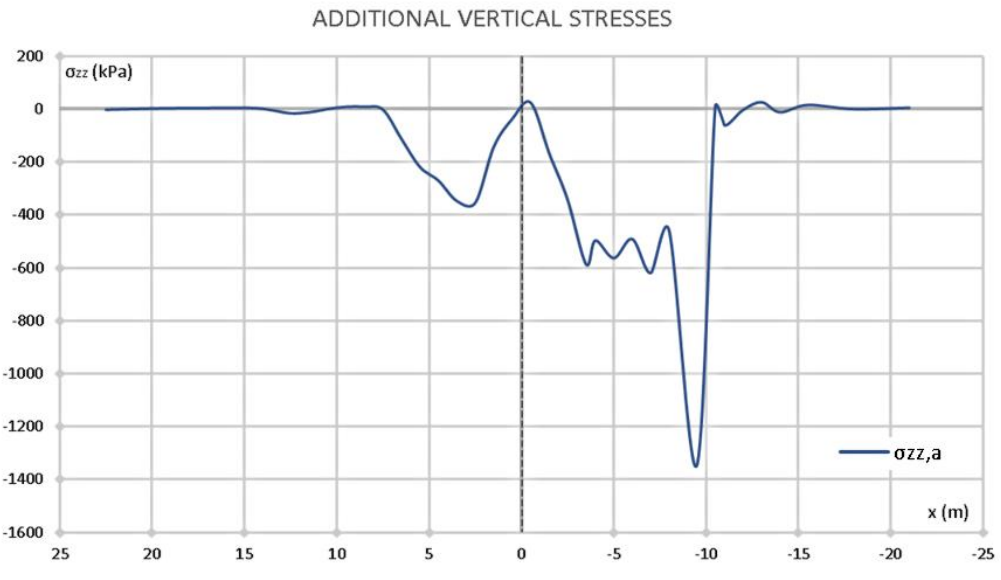

b)

Figure 3.21 Distribution of a) total vertical stresses and b) additional vertical stresses on soil surface for 95%G, 90%S_u

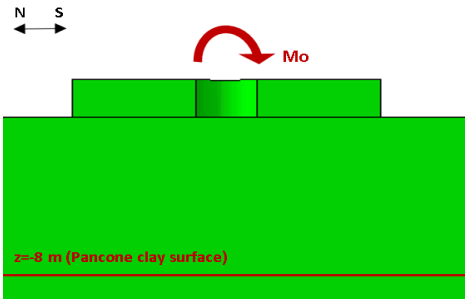

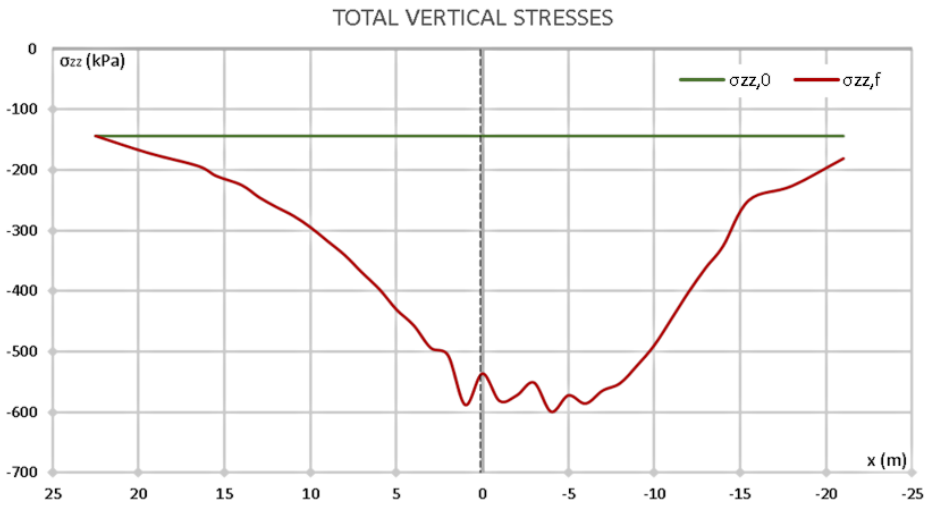

a)

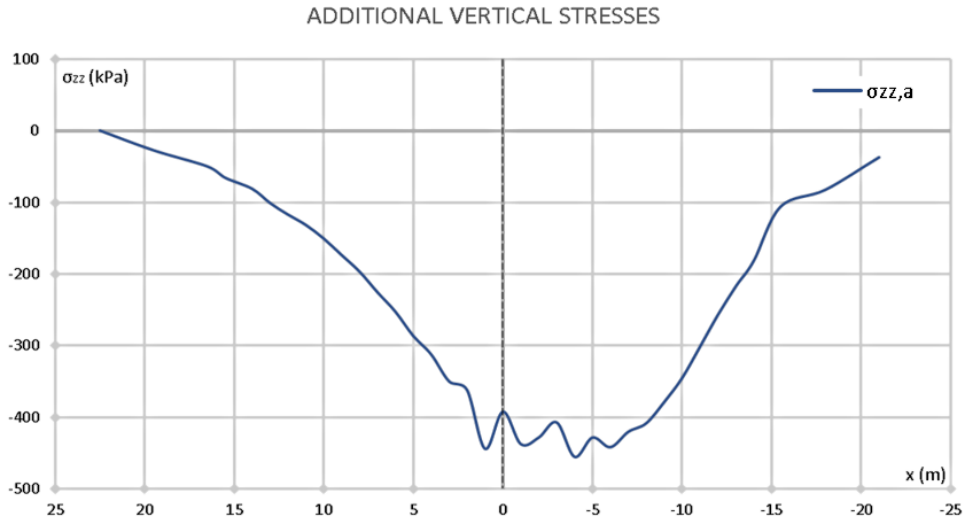

b)

Figure 3.22 Distribution of a) total vertical stresses and b) additional vertical stresses on Pancone clay surface for 95%G, 90%S_u

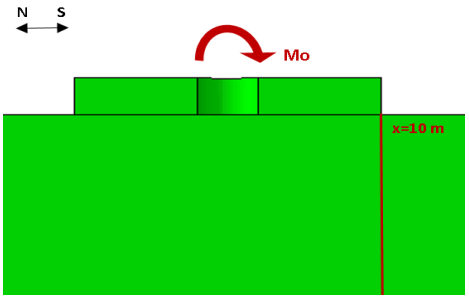

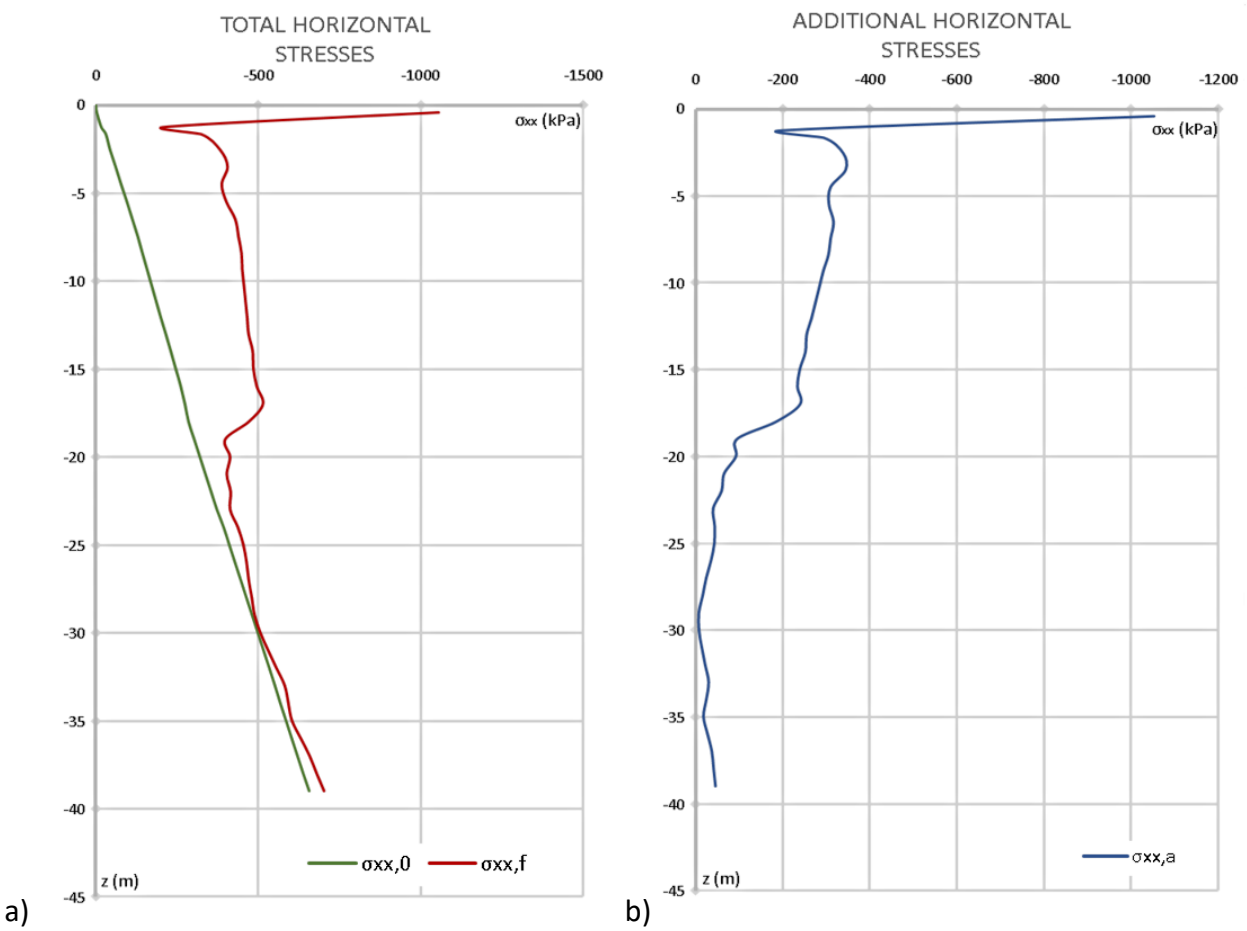

Figure 3.23 Distribution of a) total horizontal stresses and b) additional horizontal stresses with depth for 95%G, 90%S_u

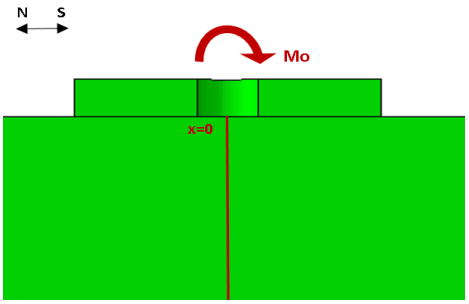

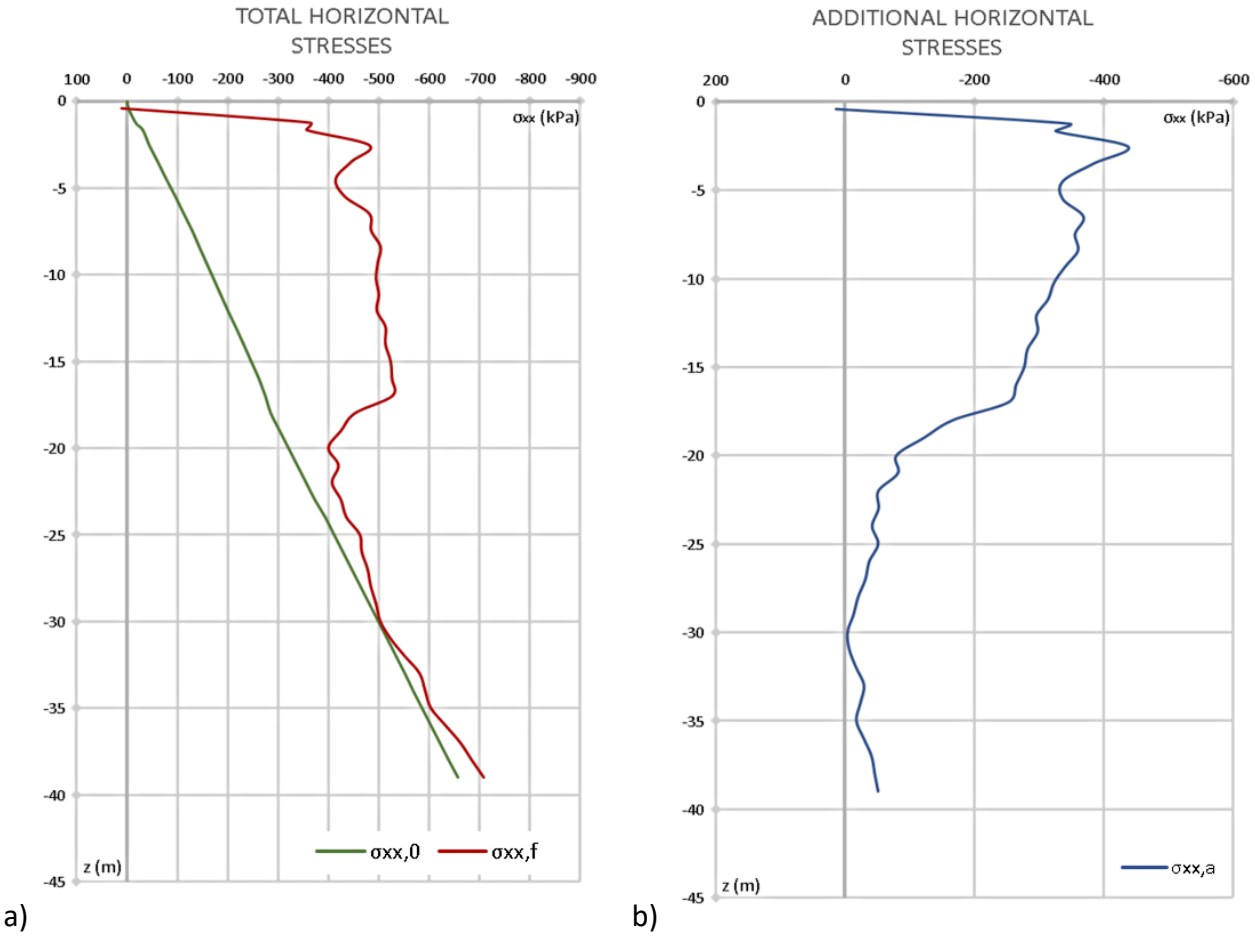

Figure 3.24 Distribution of a) total horizontal stresses and b) additional horizontal stresses with depth for 95%G, 90%S_u

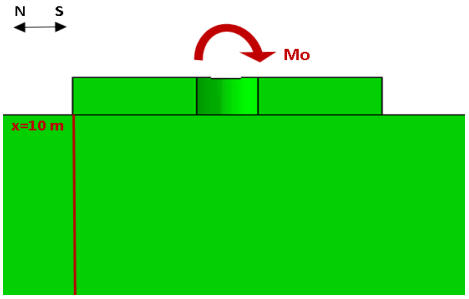

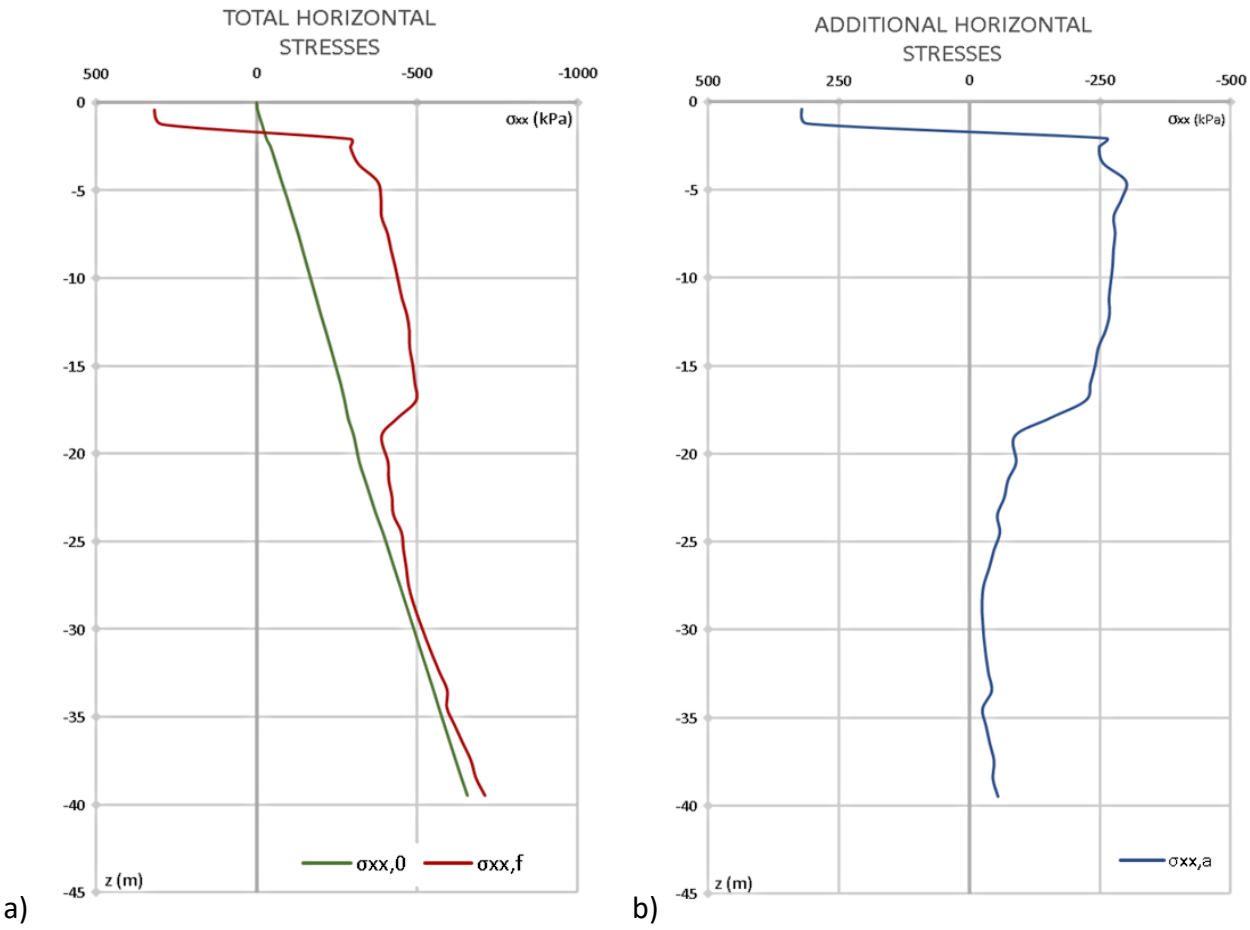

Figure 3.25 Distribution of a) total horizontal stresses and b) additional horizontal stresses with depth for 95%G, 90%S_u

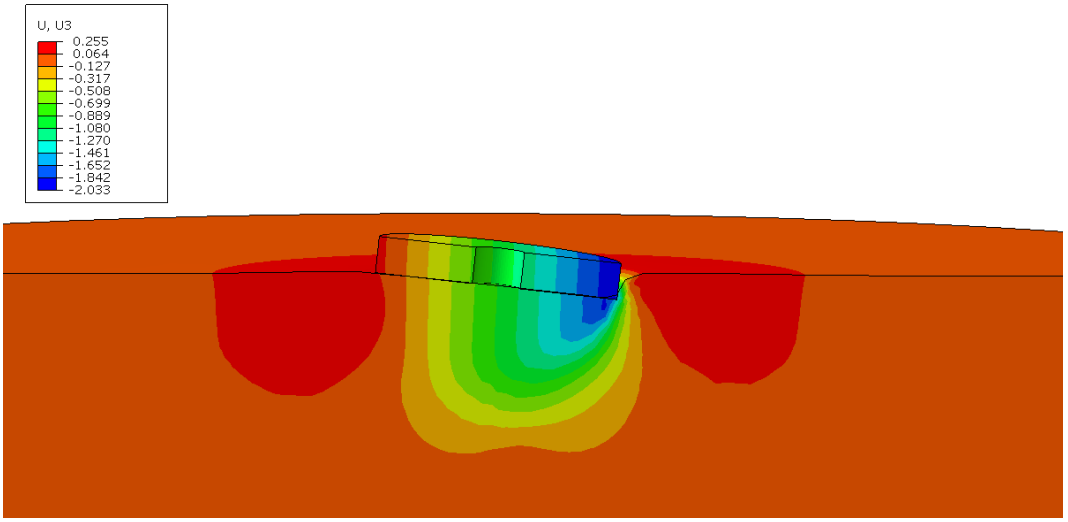

Figure 3.26 Deformed shape of the surface of the soil for 95%G, 90%S_u as depicted from Abaqus with contours settlement

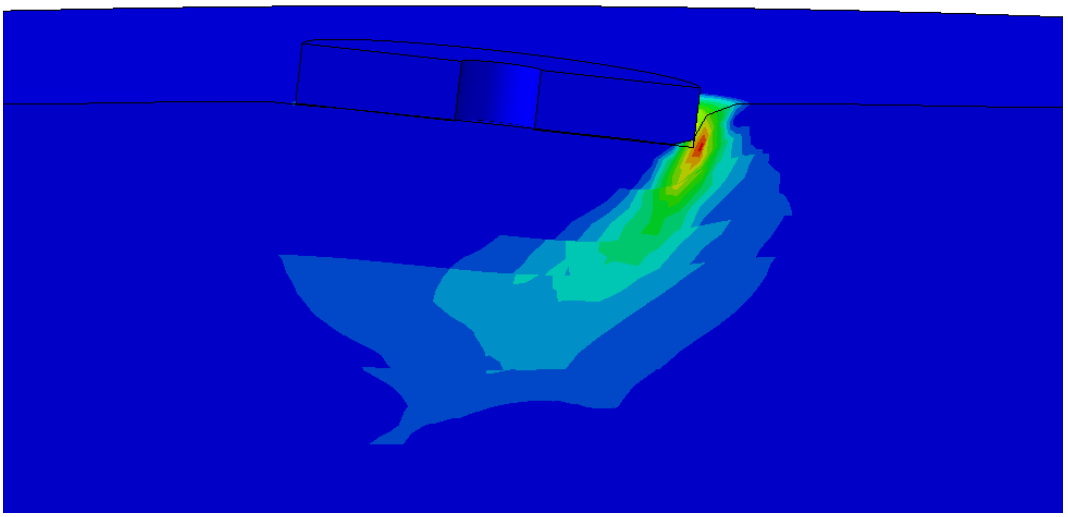

Figure 3.27 Zone of fully mobilized strength for 95%G, 90%S_u as depicted from Abaqus with contours

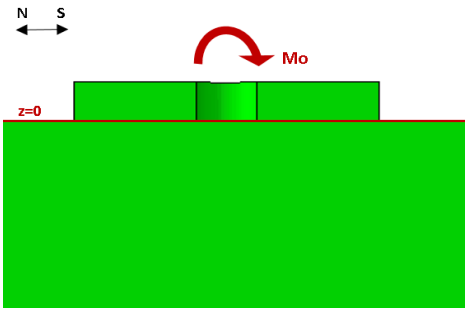

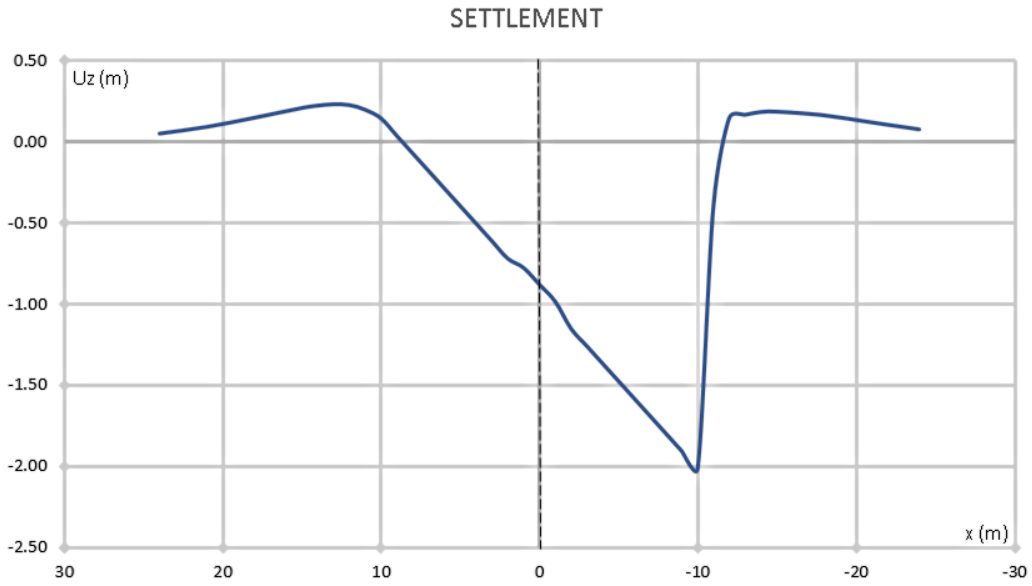

Figure 3.28 Settlement of the surface of the soil for 95%G, 90%S_u

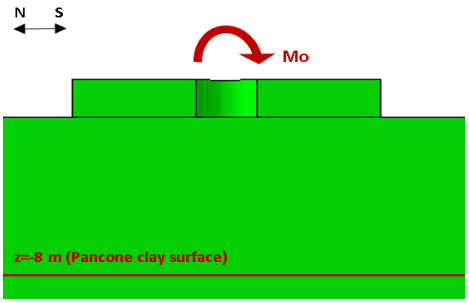

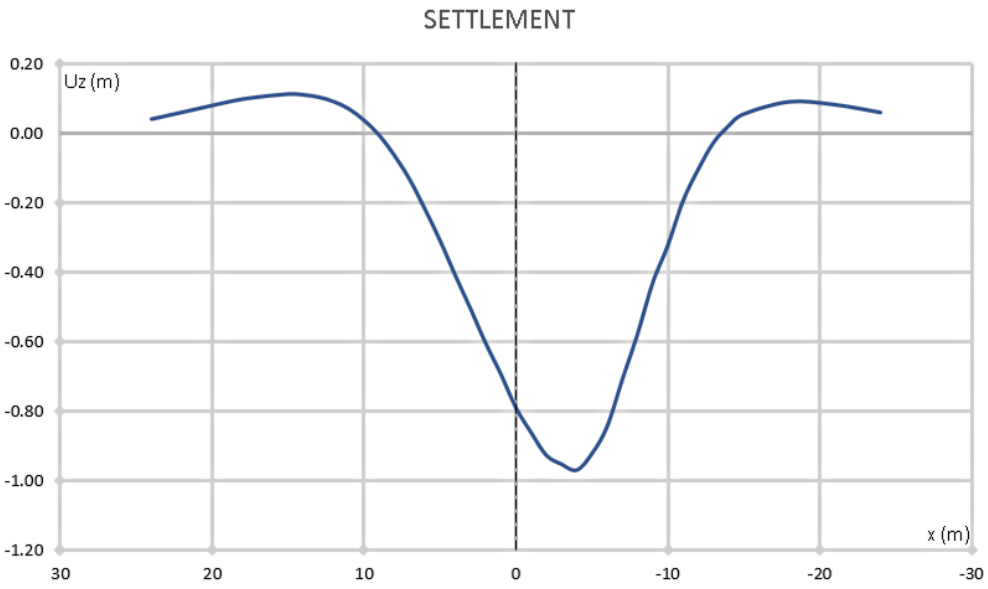

Figure 3.29 Settlement of the surface of Pancone clay for 95%G, 90%S_u

CHAPTER 4
CONCLUSIONS

The 3D simulation of the Tower of Pisa and its subsoil and the analysis of its behavior using the Finite Element Method with Abaqus code provides a reliable way to obtain a detailed overview of the factors that mainly affect its movements and the possible failure mechanisms, as well as better understand the mechanical behavior of its subsoil. We carried out a group of elastic analyses that helped us to confirm the validity of our model and, at the same time, pointed out some important aspects of the examined problem such as the significant contribution of the Pancone clay to the movements of the Tower, since it undergoes big settlements even though its surface is found approcimately 10 m under the footing. After that, we choosed the Mohr-Coulomb constitutive model to simulate the plastic behavior of the subsoil and examine its response to the applied loads due to the Tower. The obtained results are quite close to the reality: The estimated resisting moment is similar to the overturning one resulting in a safety factor FS=1.06, while the final rotation angle is 6.17° and the final settlement is equal to 2 m. It should be noted, once again, that the soil has been consolidated under the weight of the superstructure, therefore its strenght has increased. As observed by the resulting stresses and deformations of the soil, the Tower is not in danger due to lack of subsoil strength and a plastic type of failure is rather not possible. The height of the Tower together with its inclination and the subsequent differential settlements of the soil that goes on within singnifficant depth (Pancone clay) suggest that the Tower of Pisa is threatened by the phenomenon of leaning instability.

REFERENCES

- J. B. Burland, M. Jamiolkowski and C. Viggiani (2003). “The stabilization of the Leaning Tower of Pisa”, Soils and Foundations
- J. B. Burland, M. Jamiolkowski and C. Viggiani (2015). “Underexcavating the Tower of Pisa: Back to Future”, Geotechnical Engineering Journal of the SEAGS & AGSSEA
- J. B. Burland (2004). “THE LEANING TOWER OF PISA REVISITED”
- J. B. Burland, M. Jamiolkowski and C. Viggiani (2009). “Leaning Tower of Pisa: Behavior after Stabilization Operations”, International Journal of Geoengineering Case Histories
- D. Lo Presti, M. Jamiolkowski, M. Pepe (2003). “Geotechnical characterization of the subsoil of Pisa Tower”
- A.K.L. Kwong, C.K. Lau, C.F. Lee, C.W.W. Ng, P.L.R. Pang, J.-H Yin, Z.Q. Yue (2001). “Soft Soil Engineering”
- T. S. Tan, K. K. Phoon, D. W. Hight, S. Leroueil (2003). “Characterization and Engineering Properties of Natural Soils”
- J. B. Burland (1990). “On the compressibility and shear strength of natural clays”, Geotechnique
- D. M. Potts, Lidija Zdravkovic, Lidija Zdravković (2001). “Finite Element Analysis in Geotechnical Engineering: Application”
- M. Jamiolkowski, R. Lancellotta, C. Pepe (1993). “Leaning Tower of Pisa — Updated Information”
- G. Macchi, M. Eusebio, G. Ruggeri, M. Moncecchi. “Structural assessment of Leaning Tower of Pisa”
- A. Papakonstantinou (2014). “Static and Dynamic Stability of the Leaning Tower of Pisa”
- R. D. Holtz, W. D. Kovacs (1981). “AN INTRODUCTION TO Geotechnical Engineering”
- R. O. Davis, A. P. S. Selvadurai (2002). “Plasticity and Geomechanics”
- G. Barnes. “Εδαφομηχανική, Αρχές και εφαρμογές”

- Γ. Γκαζέτας, Ι. Αναστασόπουλος, Ε. Γαρίνη (2013). “Αλληλεπίδραση Εδάφους-Κατασκευής”
- Γ. Γκαζέτας (2008). “Σημειώσεις ΕΔΑΦΟΜΗΧΑΝΙΚΗΣ”
- Β. Ν. Γεωργιάννου (2012). “ΕΙΔΙΚΑ ΘΕΜΑΤΑ ΕΔΑΦΟΜΗΧΑΝΙΚΗΣ”